Flow Technical Report No. 448

AN AUTONOMOUS OCEAN INSTRUMENT PLATFORM DRIVEN VERTICALLY BY THE CURRENT

D. C. Echert, E. W. Geller, G. B. White
Flow Research, Inc.
21414-68th Avenue South
Kent, Washington 98032

and

J. H. Morison
Polar Science Center
University of Washington
Seattle, Washington

July 1988

Phase II Final Report
for Period Sept 86 - May 88
Contract No. N-00014-86-C-0816

Prepared for

OFFICE OF NAVAL RESEARCH
800 North Quincy Street
Arlington, VA 22217

Unclassified
SECURITY CLASSIFICATION OF THIS PAGE

ADA198226

REPORT DOCUMENTATION PAGE

Form Approved
OMB No 0704-0188

1a. REPORT SECURITY CLASSIFICATION Unclassified	1b. RESTRICTIVE MARKINGS
2a. SECURITY CLASSIFICATION AUTHORITY	3. DISTRIBUTION/AVAILABILITY OF REPORT Approved for Public Release; Distribution Unlimited
2b. DECLASSIFICATION/DOWNGRADING SCHEDULE	
4. PERFORMING ORGANIZATION REPORT NUMBER(S) Flow Research Report No. 448	5. MONITORING ORGANIZATION REPORT NUMBER(S)
6a. NAME OF PERFORMING ORGANIZATION Flow Research, Inc. 6b. OFFICE SYMBOL (If applicable)	7a. NAME OF MONITORING ORGANIZATION
6c. ADDRESS (City, State, and ZIP Code) 21414 68th Ave. South Kent, Washington 98032	7b. ADDRESS (City, State, and ZIP Code)
8a. NAME OF FUNDING/SPONSORING ORGANIZATION Office of Naval Research 8b. OFFICE SYMBOL (If applicable) N00014	9. PROCUREMENT INSTRUMENT IDENTIFICATION NUMBER N00014-86-C-0816
8c. ADDRESS (City, State, and ZIP Code) Department of the Navy 800 N. Quincy Street Arlington, Virginia 22217-5000	10. SOURCE OF FUNDING NUMBERS PROGRAM ELEMENT NO. / PROJECT NO. / TASK NO / WORK UNIT ACCESSION NO.

11. TITLE (Include Security Classification)

An Autonomous Ocean Instrument Platform Driven Vertically by the Current

12. PERSONAL AUTHOR(S)
D.C. Echert, E.W. Geller, G.B. White, and J.H. Morison

13a. TYPE OF REPORT	13b. TIME COVERED	14. DATE OF REPORT (Year, Month, Day)	15. PAGE COUNT
Final	FROM Sept 86 TO May 88	July 1988	58

16. SUPPLEMENTARY NOTATION

17. COSATI CODES			18. SUBJECT TERMS (Continue on reverse if necessary and identify by block number)
FIELD	GROUP	SUB-GROUP	ARGOS, Oceanographic Instrument, Buoy, Profiler, Salinity, Hydrofoil, Reynolds Number, Temperature

19. ABSTRACT (Continue on reverse if necessary and identify by block number)

This report describes the development and initial field test results of the Autonomous Ocean Profiler (AOP). The AOP is an oceanographic instrument platform for measuring profiles of physical, thermodynamic, and biological properties in the ocean. The profiler employs a hydrodynamic lift device to "fly" the instrument package up and down the water column along a taut vertical cable. Because the local currents drive the platform's vertical motion, power requirements are low and, therefore, long, unattended deployments are possible. By using ARGOS or GOES satellite retrieval networks, the system can supply near-real-time data. The system provides profile data at very high vertical resolution in contrast to

(Continued on Reverse)

20. DISTRIBUTION/AVAILABILITY OF ABSTRACT	21. ABSTRACT SECURITY CLASSIFICATION
☒ UNCLASSIFIED/UNLIMITED ☐ SAME AS RPT. ☐ DTIC USERS	Unclassified

22a. NAME OF RESPONSIBLE INDIVIDUAL	22b. TELEPHONE (Include Area Code)	22c. OFFICE SYMBOL
Robert Obrochta	(202)696-4720	N00014

DD Form 1473, JUN 86 *Previous editions are obsolete.*

19. Abstract (Continued)

conventional buoys, which gather data only at fixed sensor depths. Because only a single set of sensors is required to cover the vertical range desired, the system is low-cost and, for many applications, expendable. The initial deployment configuration is as an Arctic drifting buoy. A satellite retransmission buoy is placed on the sea ice surface with the cable suspended below the ice. Conductivity, temperature, and depth information are gathered over a depth range of 0 to 300 m. Data are internally recorded and are relayed to the surface buoy through an inductive communication link for transmission via satellite. Initial test results from Puget Sound and from an Arctic test are described.

ACKNOWLEDGEMENTS

This work was sponsored by the Office of Naval Research (ONR) under contract No. N00014-85-C-0675. Our thanks to Mr. Robert Obrochta of ONR for his many thoughts and suggestions concerning the AOP development. Our thanks also to Sea Bird Electronics, Inc., for their technical assistance during the project and to Mr. Mike Welch of the University of Washington's Polar Science Center for his outstanding support during the Arctic field test. The AOP mechanical design was engineered by Mr. Sam Smith.

TABLE OF CONTENTS

LIST OF FIGURES

LIST OF FIGURES (CONT.)

LIST OF TABLES

1. INTRODUCTION

Within the oceanographic community there is a need for an automatic, unattended instrument system capable of measuring profiles of ocean properties over long periods of time. The profiling system must be low in cost so that it can be expendable for most applications. An additional requirement for the system is that it be small and lightweight so that many units can be carried on a deployment aircraft or vessel.

An instrument system with both profiling capability and long endurance is important for two reasons: (1) to provide data on seasonal changes in regions where, due to logistical constraints, it is impossible to attend or service the equipment, and (2) to provide high vertical resolution, which is unobtainable with individual sensors at fixed depths. Such a system will permit ocean investigators to obtain higher quality data at lower cost. Flow Research, Inc., has developed the Autonomous Ocean Profiler (AOP)* to meet this need.

The AOP development has focused initially on providing a system for the Arctic. This application was singled out because the Arctic provides severe logistical requirements on any data-gathering program. Thus, the cost savings derived from the use of an AOP buoy relative to alternative systems will be great. Additionally, there is increasing interest by both Naval and non-military researchers in obtaining Arctic oceanographic data over long time periods.

For the Arctic application, the device is suspended from a drifting ice floe. The data are relayed by satellite from a buoy at the ice surface. In this way the system is similar to the existing SALARGOS [1] buoy that it is intended to replace. The SALARGOS buoy consists of an aluminum tube containing the data acquisition and transmission electronics and enough alkaline batteries to power the buoy for one year. The buoy is placed at the ice surface, and temperature and conductivity sensor pairs are suspended below on a multiconductor cable, each pair gathering data at a different depth. Three to six sensor pairs are attached to the cable. Although the SALARGOS buoys are capable of producing valuable oceanographic data, the use of fixed-depth sensors severely limits vertical resolution and increases system cost. The AOP improves upon the SALARGOS buoy concept through active profiling; the fixed string of sensor pairs is replaced with a single sensor package that moves vertically through the water.

*Autonomous Ocean Profiler and AOP are trademarks of Flow Research, Inc.

2. CONCEPTS AND TECHNICAL CONSIDERATIONS

In this section, the specific technical requirements for developing a practical AOP are discussed. These include hardware concepts, sampling and instrumentation requirements, and ocean conditions.

2.1 Concepts

The initial task of the AOP development was to select a suitable method of providing automatic profiling. Possible schemes included the following: (1) a variable buoyancy float, (2) a battery-operated, counterbalanced winch, and (3) a controlled, hydrodynamic lift device. The first scheme involves inflating and deflating a bladder to raise and lower the sensors. This technique is employed in the Cyclesonde [2], which uses compressed gas, and in the Profiling Current Meter (PCM) [3], in which an electric pump is used. In the second scheme, a small battery-operated capstan raises and lowers the instrument package. The package is counterbalanced by a dead weight to minimize power requirements. The third strategy employs a hydrofoil to "fly" the instrument package up and down. This can be implemented with a tethered hydrofoil (similar to a kite), as in the towed application of Katz and Nowak [4], or by using a taut vertical cable on which the hydrofoil rides up and down. For either hydrofoil deployment strategy, the platform uses the prevailing currents to produce hydrodynamic lift, and the only power requirement is for rotation of the hydrofoil to change the lift direction.

Based on our review of these techniques, the hydrofoil using the taut cable was selected as the most feasible and most likely to provide longer endurance for a given package size. It does have the drawback of a less certain profiling capability due to the need for some minimum relative water velocity. However, oceanographic conditions in the Arctic change slowly relative to more temperate regions. Therefore, for the Arctic application, regularity of sampling and high data rates may be sacrificed for endurance and reliability. The taut cable configuration was selected over the kite-type profiler because, unlike the kite, it is not limited in vertical profiling range.

A sketch of the Arctic AOP concept is shown in Figure 1. The vertical cable along which the platform is guided is suspended from floating ice. Data are transmitted to a surface buoy, which retransmits via satellite link.

For non-Arctic applications, the AOP can be either bottom-anchored with a mid-depth or near-surface float or suspended from an open-ocean surface drifting buoy. Because the AOP is not rigidly fixed to the vertical cable, it is isolated from the wave-induced vertical motion of the surface buoy.

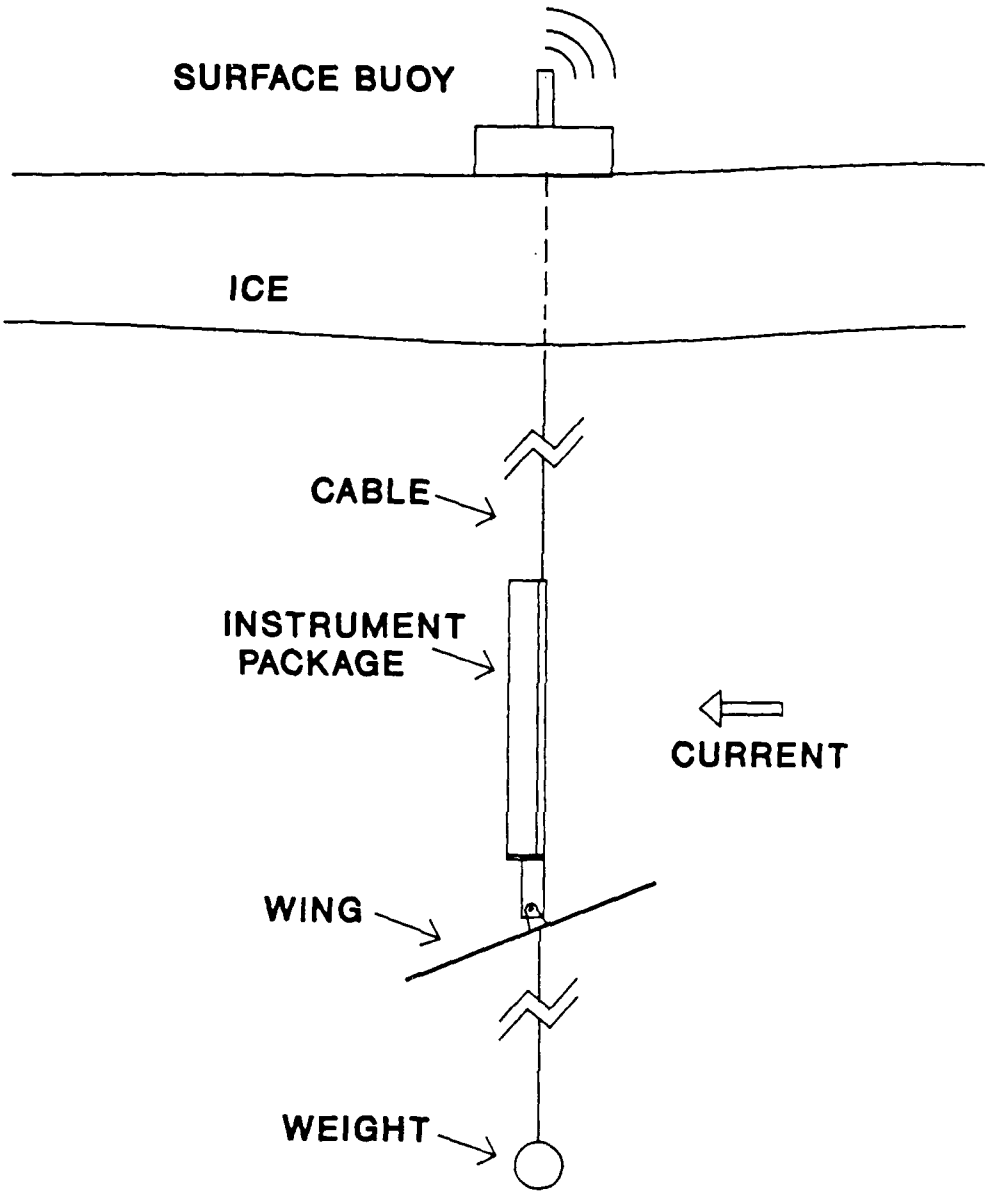

Figure 1. Concept for the Arctic Autonomous Ocean Profiler (AOP).

2.2 Sampling Requirements

A design objective for the Arctic AOP is to provide at least one good daily profile of temperature, salinity, and pressure over a period of one year. The vertical resolution must be as fine as 2 m, and the depth range up to 300 m. Temperature, conductivity, and pressure must be recorded to 16-bit accuracy; this has proven to be an adequate requirement for previous Arctic buoy deployments. For each sample requiring temperature, conductivity, pressure, and time (at 8-bit accuracy), the minimum data rate, n_{min}, is

$$n_{min} = (150 \text{ samples/cast})\ (56 \text{ bits/sample}) = 8400 \text{ bits/cast.} \quad (1)$$

When used in an unattended mode, it is assumed that the data will be telemetered from the buoy using the ARGOS system. As a rule of thumb for the Arctic, a single ARGOS satellite makes one pass every 101 minutes or 14.25 passes per day, and during each pass a buoy can make 10 good transmissions of 256 bits at 1-minute intervals. This results in a maximum ARGOS data rate of 36,480 bits per day. Thus, the number of bits, n_{min}, required per cast (or per day) can be transmitted through ARGOS 4.3 times per day. In fact, because there are usually two satellites operating, if the equivalent of 4 casts per day were transmitted, they would ideally all be received twice.

A practical sampling strategy calls for sampling 4 casts per day. Under optimum conditions, an average time resolution of 6 hours would then be obtained with a safety factor of 2. In the worst case, one profile each day would get through ARGOS with a safety factor of 4.

2.3 Instrumentation Requirements

For the Arctic mission, a simple sensor package was selected that has conductivity, temperature, and pressure sensors. The AOP can be fitted with other types of oceanographic sensors depending on the mission of the platform. Even with this limited suite of sensors, the AOP is able to measure current speed profiles. Current speed can be obtained from the vertical velocity of the platform, as measured by the change in pressure with time. Therefore, the platform serves as a low-cost current profiling instrument. The measurement error caused by deviation from neutral buoyancy can be minimized by averaging the AOP velocity over one or more ascent/descent cycles. Current direction can be sensed with the addition of an on-board compass.

In addition to the sensors, the on-board payload includes the following:

- o A microprocessor for directing the operation of the AOP.
- o Signal conditioning for the sensors.
- o A telemetry link to the surface.
- o Motor and controls to change ascent/descent.
- o Batteries.

To meet the long-term deployment requirement, all of the components must be low power.

2.4 Ocean Conditions

Obviously, the world's oceans exhibit a wide variety of conditions. Primarily Arctic applications are addressed in this study, although the profiler could be used elsewhere with modification. Because of the low current velocities there, the Arctic presents the most severe test of the feasibility of a hydrofoil profiling system. The most likely changes for use outside the Arctic would be in the mooring configuration rather than in the instrument itself.

For Arctic applications, the following environmental and performance parameters apply:

- o The profiler should be able to sample the upper 300 m of the water column.
- o The profiler should be able to operate over a current speed range of 3 to 40 cm/s.
- o The profiler must be able to generate enough lift to overcome its weight in water, which will vary due to temporal and spatial changes in the water density of up to 0.4 percent.
- o The system must operate at low temperatures corresponding to the freezing point of seawater.
- o The system must be able to withstand air temperatures of -40 degrees C during deployment.

The 300-m depth range extends through the surface mixed layer and down to the Atlantic layer in the Arctic Ocean. The speed range is typical of relative water velocities that might be expected in the Arctic. An average relative current speed of 6 cm/s is typical for the Arctic Basin, and relative currents are rarely below 3 cm/s for extended periods. The estimate of a maximum seawater density change of 0.4 percent due to temporal and spatial variations is based on previous oceanographic observations in the Arctic. An average Arctic density profile, showing expected annual deviation compiled from various sources [5,6], is shown in Figure 2.

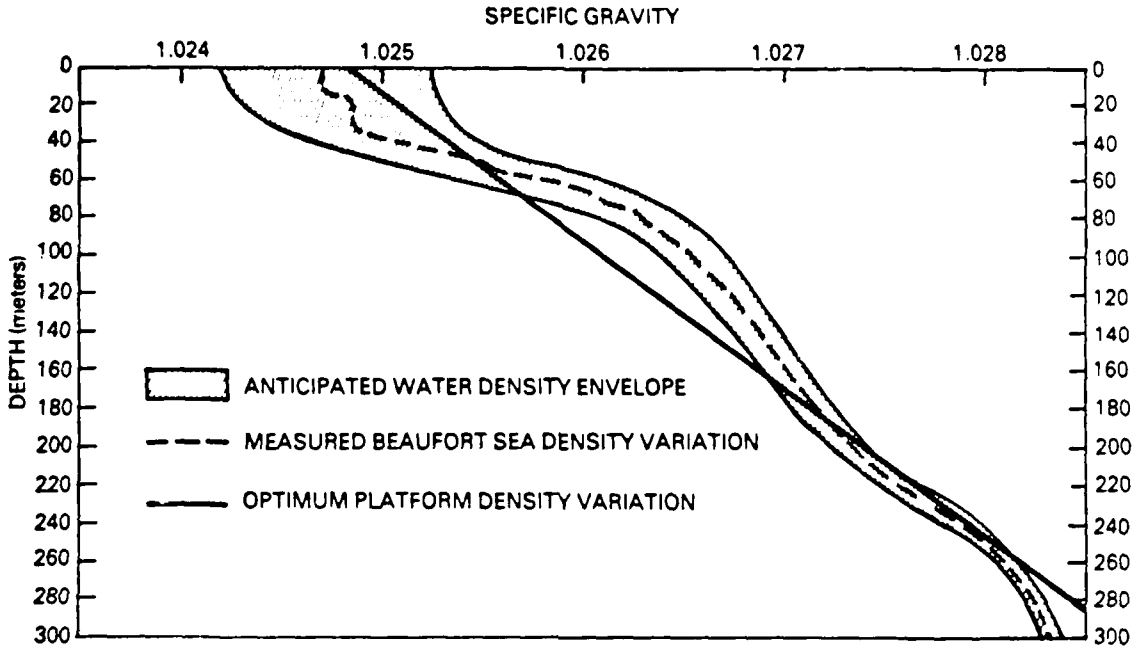

Figure 2. Arctic seawater density envelope. **The optimum linear density variation of the AOP with depth is shown.**

3. DEVELOPMENT OF THE AOP DESIGN

The major goals that governed the design of the AOP are the following:

- o The platform must be able to traverse the cable for current speeds as low as 3 cm/s within the ocean density envelope specified in Figure 2.
- o The platform must be strong enough to withstand loads at current speeds up to 60 cm/s.
- o The platform should have a small overall size and be able to fit through a 30 cm hole in the ice.
- o It should be of simple, inexpensive construction.

The ways in which these goals influenced significant aspects of the design are described below.

3.1 Wing Shape

A delta wing was chosen for the lifting shape of the hydrofoil because of the following advantages not inherent in a conventional wing shape:

- o It exhibits no degradation in the maximum lift coefficient at very low Reynolds numbers.
- o It is effective at very low aspect ratios.
- o The airfoil shape is not important--a flat plate will do.

These three features result from the fact that a highly swept delta wing at high angles of attack relies on vortex lift, an entirely different lift mechanism than that for a conventional wing. Vortex lift is created by large-scale vortices above the wing that reduce the pressure. These vortices are generated by separation along a highly swept wing leading edge. A sharp leading edge is not detrimental and, in fact, promotes separation at the leading edge. The airfoil shape is nearly irrelevant at high angles of attack, the only requirement being that the leading edge be sufficiently sharp to fix separation there. A flat-plate airfoil is quite satisfactory. Since the entire vortex lift phenomenon is driven by separation at the leading edge, and since this occurrence does not depend upon the Reynolds number if the leading edge is sharp, the lift for high angles of attack of a highly swept delta wing does not drop off at the very low Reynolds numbers associated with operation of the profiler.

The preceding features of the delta wing translate into several advantages. The ability to use a thin flat-plate airfoil leads to a simple, inexpensive wing construction. The wing size required for operation in very low currents is smaller than for a traditional wing, for which Reynolds number effects reduce maximum lift. And, finally, the lower aspect ratio would

translate into less wing span for the required wing area. This, coupled with the ability to use a thin, flat-plate wing, allows it to be compactly rolled up for deployment through a much smaller hole in the ice than would be possible with a conventional wing shape.

Theoretical considerations suggest that the lifting performance of a delta wing at high angles of attack is independent of Reynolds number. This has been experimentally confirmed at Reynolds numbers very low for aircraft [7] but still several orders of magnitude greater than for AOP operation. There was some concern that the maximum lift of the delta wing would be reduced at the very low Reynolds numbers (on the order of 1000) where the AOP would operate. Therefore, a series of scale model tests was conducted in the Flow Research, Inc., tow tank to evaluate the delta wing performance. Details of the tests are presented elsewhere [8]. The test results confirmed the theory; no degradation in performance was seen.

3.2 Lifting Requirements and Impact on the Design and Sizing

If the AOP is neutrally buoyant, it then can generate sufficient lift to profile, no matter how small the wing and how low the current. However, neutral buoyancy is not possible at all times because of spatial and temporal variations in water density and changes in platform density from water absorption during long-term deployment.

It is desirable to minimize the wing area to facilitate handling and deployment. The wing size is determined from the maximum expected weight of the AOP in water. The weight in water is proportional to the displaced volume of the platform and the deviation of the platform density from the water density. Therefore, to minimize the required wing area, it is desirable to minimize the displaced volume of the platform.

Deviations of platform density from water density over the vertical range to be profiled also can be minimized by using a pressure/volume compensator to reduce the displaced volume of the platform as it descends into the more dense water (shown in Figure 2). The AOP will carry a spring-loaded bellows to obtain a volume reduction with depth. For compensation that is linear with depth, the maximum density difference between the AOP and the ocean is reduced by a factor of 2 for the ocean density difference shown in Figure 2. This translates into a wing area reduction by a factor of 2.

3.3 Threshold Speed and Vertical Velocity

The amount of lift that is generated by the wing from the current is proportional to the wing area. The size of the wing can be tailored to meet the expected currents at a given site. For example, doubling the wing span will result in a twofold reduction in the threshold speed, the minimum current necessary for vertical motion.

Lift is also a function of wing angle of attack. For example, the AOP wing shape at an angle of attack of 30 degrees produces 27 percent more lift than at an angle of attack of 22 degrees. At an angle of 22 degrees, it can be shown that the wing approaches a vertical velocity of 41 percent of the current speed if drag is neglected. At a 30-degree pitch angle, this limiting speed ratio is 57 percent of the current speed.

Higher vertical velocities can be achieved by using higher pitch angles. For example, a pitch angle of 70 degrees could produce a vertical velocity of 2 to 3 times the current velocity. The disadvantage is that the minimum threshold speed would be increased, because at zero vertical velocity the 70-degree angle of attack would stall the wing, producing little lift. One could use a variable-pitch angle mechanism where the angle increases as the vertical velocity of the AOP increases. Then, the vertical velocity could be monitored and analyzed on-board, and the wing angle adjusted appropriately by the wing rotation motor. The disadvantage of this approach is increased mechanical and electronic complexity.

4. AOP FINAL DESIGN

The final prototype design of the AOP is shown in Figure 3 (with the fairing for the instrumentation housing removed). The basic elements of the AOP are as follows:

- o Sensor and electronics package. This includes the motor controller, telemetry system electronics, and batteries.
- o Cable rollers.
- o Drive motor and communications coil housing.
- o Wing, linkage mechanism, and support strut.

A discussion of these basic elements and other final design details, including system specifications, is given in this section.

4.1 Sensors

A modified Sea-Bird Electronics, Inc., SEACAT profiler is used as the basis of the instrumentation package. This unit includes a conductivity sensor, a temperature sensor, a Digiquartz pressure sensor, and a microprocessor-controller with CMOS RAM memory.

4.2 Data Storage and Telemetry

Data are telemetered to either a surface buoy for retransmission or to a surface recording device. An inductive link is used to transmit the data up the vertical supporting cable. In addition, a one-month set of data can be stored on-board the AOP.

4.3 Ascent/Descent Control

The hydrofoil's pitch angle controls whether the platform moves up or down the guide cable. A gear motor rotates the hydrofoil to either a fixed nose-up or fixed nose-down angle. The on-board microprocessor determines when the platform's direction is to be reversed. The controller compares periodic pressure measurements with limit values stored in memory, which represent the range over which the AOP is to operate. When the AOP reaches one of these limit values, the angle of the hydrofoil is reversed. The AOP also can be set to reverse the wing angle after obtaining a user-specified number of data scans.

4.4 Through-Ice Deployment

It is desirable to minimize the hole size required for through-ice deployment of the AOP. The wing, which is built from a thin sheet of polycarbonate plastic, can be rolled to a diameter less than 30 cm. For deployment, the wing linkage is extended to permit the wing to rotate to a position parallel to the instrumentation housing, as shown in Figure 4a. The wing is rolled

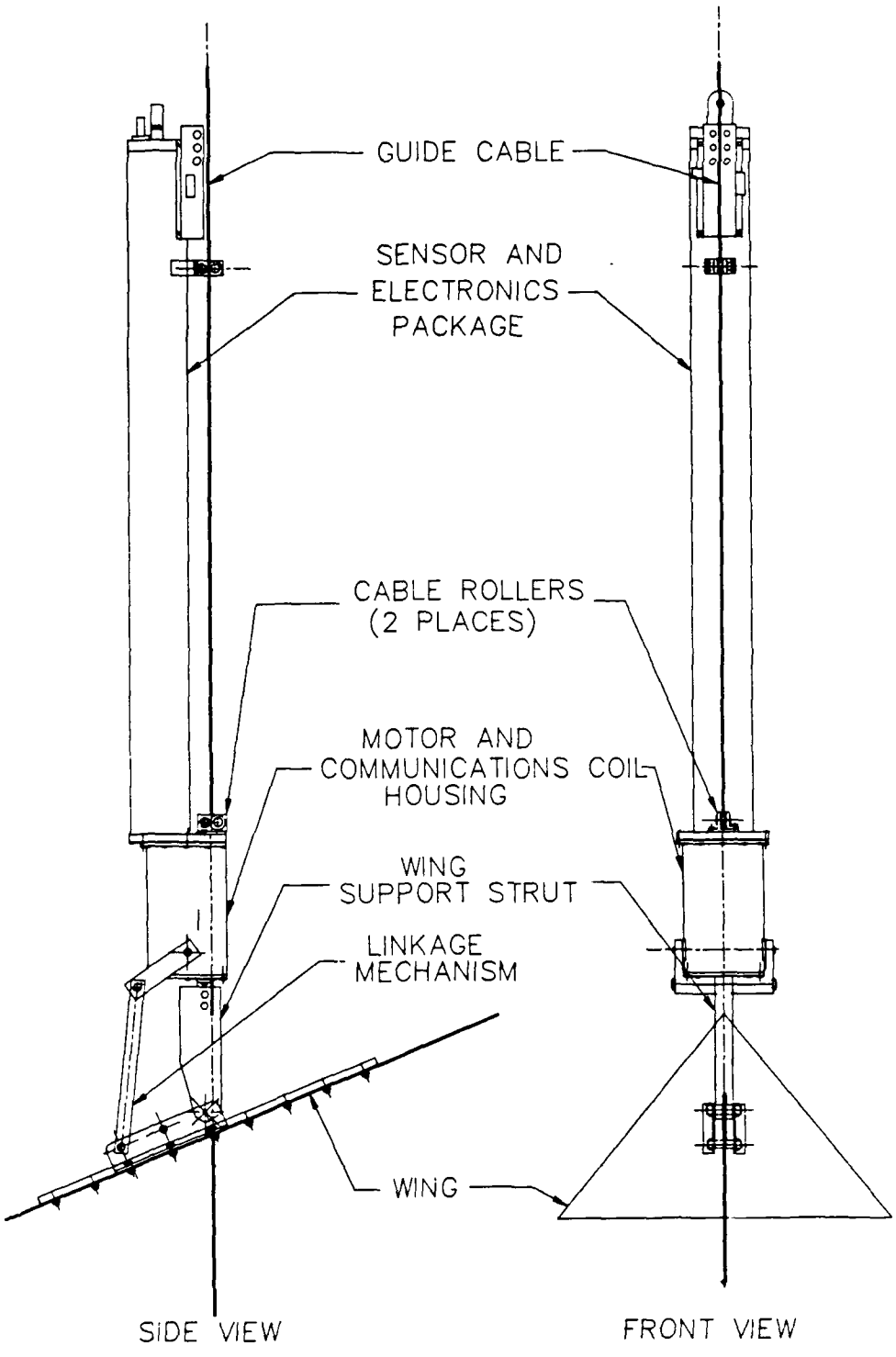

Figure 3. **Field prototype design for the AOP.**

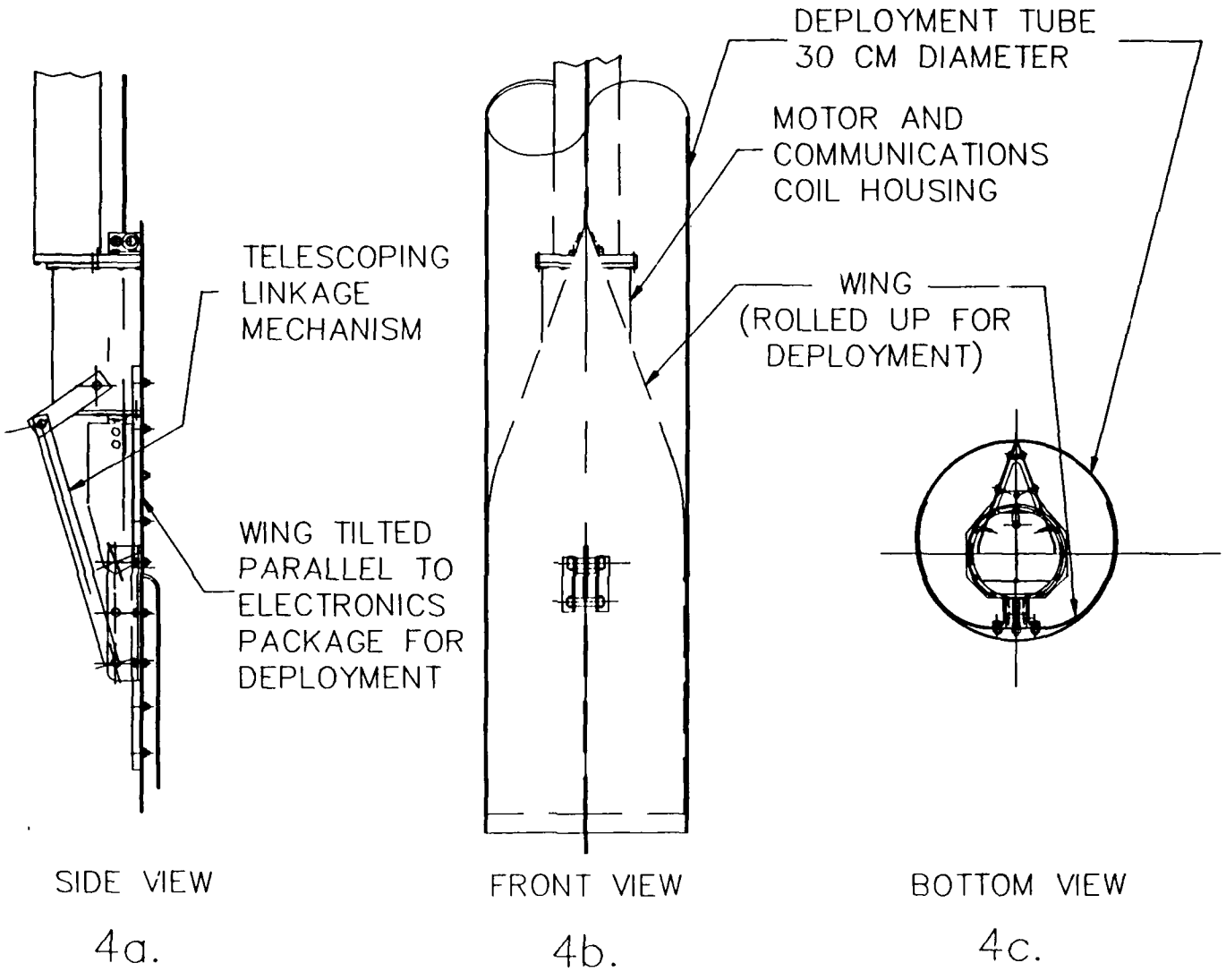

Figure 4. **AOP configured for through-ice deployment. Figure 4a shows the wing tilted vertically, Figure 4b is with the wing rolled and inserted into the deployment tube. The bottom view, 4c, includes the fairing on the instrument housing.**

around the housing and is held in place with a tube, as shown in Figure 4b. Once inserted through the ice, the tube is withdrawn, allowing the wing to extend. At the first nose-down command, the linkage is retracted to its normal operating length and is fixed in position by a detent.

4.5 System Specifications

General AOP specifications for an unattended Arctic mission are given in Table 1.

TABLE 1. System Specifications.

Weight in Air:	18 kg
Weight in Water:	0 ± 25 gm
Total Length:	2.1 m
Wing Area:	0.29 m^2
Minimum Current for Profiling:	3 cm/s
Maximum Vertical Velocity:	50 percent of current speed (approx.)
Endurance:	1 year
Depth Rating:	400 m
Data Rate:	600 daily measurements of conductivity, temperature, and depth
Measurement Range:	
Temperature	-5 to +35 degrees C
Conductivity	0 to 7 S/m
Pressure	0 to 620 decibars
Sensor Resolution:	
Temperature	0.001 degrees C
Conductivity	0.0001 S/m
Pressure	0.006 m
Sensor Accuracy:	
Temperature	0.01 degrees C/6 months
Conductivity	0.001 S/m/month
Pressure	0.05 percent of full scale range

5. INITIAL FIELD TEST RESULTS

The results of the initial testing of the AOP are described in this section. The initial tests included threshold lift-off tests in a swimming pool, operational tests from a drifting vessel in Puget Sound, and a brief test of the system in the Arctic. These are described below.

5.1 Pool Test

The objectives for testing the AOP in a pool were (1) to measure the electrical current required to rotate the wing at selected water current speeds and (2) to test the threshold speed at selected weight conditions. A measurement of the electrical current necessary to rotate the wing is needed to define the AOP electrical power budget. It also provides an indication of the location of the wing center of pressure relative to the hinge point as a function of wing angle. If the AOP were neutrally buoyant, the threshold speed would be zero. The threshold speed of the AOP has meaning only when the buoyancy of the AOP is defined, that is, how much weight the wing must lift.

The tests were conducted in the deep end [3.7 m (12 feet)] of an Olympic-sized pool. The circulation system of the pool was turned off overnight to reduce currents in the water so that the speed of the AOP relative to the water was only a function of the speed at which the AOP was towed. A special test fixture was assembled consisting of a cable suspended from a surface float and weighted at the lower end. The AOP was then mounted on the cable. A rope and pulley system, powered by a variable-speed electric capstan, was used to tow the float across the pool. The towing speed was obtained from time and distance measurements. From one side of the pool to the other, the towing speed was constant to within 5 percent.

Electrical Current Draw Tests

The greatest force required to rotate the wing occurs when the AOP is fixed against an upper or lower stop on the cable and the wing is rotated to move away from the stop. For this condition there is no relative motion of the AOP to reduce the angle of incidence as seen by the AOP; the wing generates the maximum lift as defined by the wing angle setting. If the wing center of pressure and the hinge point were to coincide, a vanishingly small torque would be sufficient to rotate the wing. From the wind tunnel data available on a delta wing [7], it is known that the center of pressure moves very little with the angle of attack up to about 30 degrees. Some motion of the center of pressure could result from the hole in the wing for the guide cable and from flow interference caused by the wing support member. The tests were conducted to determine if these variations in the center of pressure could result in large power requirements for wing rotation.

The AOP was fixed to the guide wire just below the float so that it could not move vertically. Wires were run from the AOP wing rotation motor to a power supply and ammeter located poolside. The power requirements for wing rotation were determined by measuring the motor current necessary to turn the wing at selected water current (tow) speeds.

Motor current measurements ranged from 100 to 140 mA at 5.5 V over tow speeds ranging from 14 to 40 cm/s. Interestingly, the current drawn by the motor was not appreciably affected by the tow speed. Only the angle of the wing caused any fluctuation in the motor current. The motor current was lowest as the wing moved toward a zero angle of incidence and was highest as it moved away from this position toward the 22-degree wing stop. This observation indicates that the wing's center of pressure was located behind the wing hinge point. This is an advantage since it prevents the wing from becoming pinned to the wing stop by strong water currents when the AOP is fixed against an upper or lower guide cable stop.

Threshold Speed Tests

For the threshold tests, the AOP was weighted to be negatively buoyant. The weight in water was measured in the pool using a triple-beam laboratory balance mounted on a structure over a corner of the pool. The balance had an accuracy of 0.1 gm, but the accuracy of the resulting AOP weight was approximately 5 gm due to the large inertia of the AOP and difficulty in adjusting the balance weights.

The AOP was installed on the cable so that it rested on the cable sinker weight. The float then was towed across the pool at a selected speed. If the AOP lifted off the weight, the towing speed was reduced for the next test; if no lift-off occurred, the towing speed was increased. In this iterative manner the actual threshold speed for each weighted condition was measured.

The expression for threshold speed, V_{min}, neglecting cable friction, is [see Equations (A.4) and (A.5) in the Appendix]:

$$V_{min} = \left(\frac{2g}{C_{Lmax}} \frac{H}{S} \frac{W_d}{W} \right)^{\frac{1}{2}} \qquad (2)$$

where

g	=	gravitational acceleration
C_{Lmax}	=	maximum lift coefficient at angle of attack equal to wing pitch stop angle
H	=	displaced volume of AOP
S	=	wing area
W_d	=	AOP maximum weight in water
W	=	AOP weight in air

From this expression one can see that the threshold speed should vary as the square root of the weight in water.

The AOP was tested with no fairing or other provision for drag reduction. During the tests, the AOP oscillated from side to side, sweeping out an arc of approximately 60 degrees at a period of approximately 1 second. This motion was seen even at the lowest speeds tested. In an effort to confirm that vortex shedding from the vertical AOP housing was the cause of the motion, the wing was removed. The oscillation persisted, confirming that the instability was not due to a directional instability of the wing itself.

Threshold speeds were measured for three AOP weights: 20.8, 55, and 448 gm. These weight conditions provided threshold speeds of 5.5, 7.4, and 22.6 cm/s, respectively. These speeds are plotted against the square root of the AOP weight in Figure 5. Also shown in the figure is a line calculated from the expression given above, Equation (2), using wind tunnel data for C_L [9]. The measured threshold speed is greater than the calculated speed (neglecting cable friction) by an average of 32 percent. We estimate that cable friction would increase the threshold speed by 10 percent over the results calculated from the wind tunnel data with the assumption of no cable friction. It is thought that the remaining difference between the calculation and the measurements is due to one of two reasons. The major factor is likely the

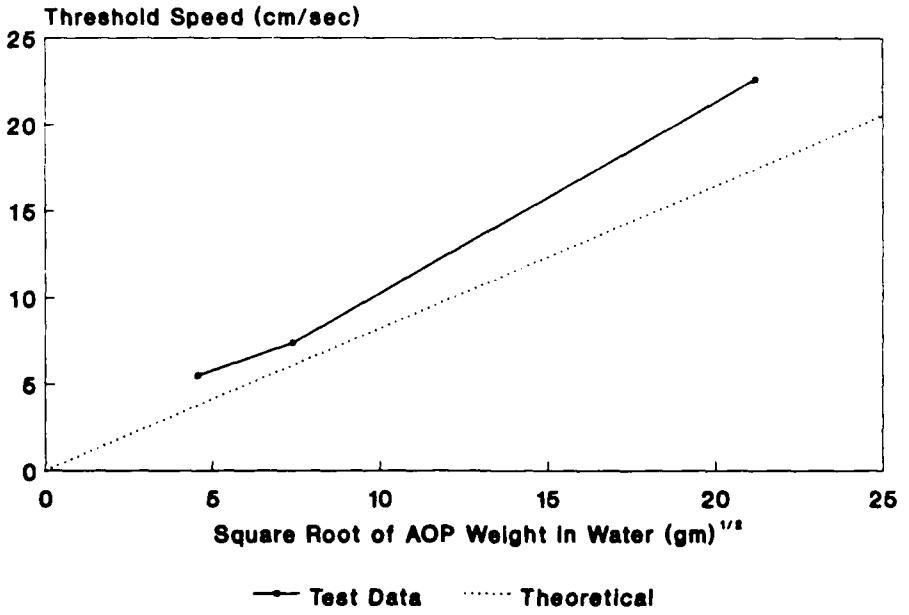

Figure 5. AOP threshold speed test results.

effects of the vortex shedding. The increased drag of the AOP due to the vortex shedding would have increased the cable friction significantly and, additionally, the oscillatory motion may have reduced the lift generated by the wing. The other possible reason is the loss of differential pressure resulting from fluid flow through the cable guide hole in the wing, a condition not present for the wind tunnel tests.

To solve the vortex shedding problem, a series of tests was conducted in the Flow Research tow tank. Various techniques of vortex reduction were applied to a vertical cylinder towed through the water. The techniques included a standard hydrodynamic fairing extending one tube diameter back from the tube; a flexible plastic fairing attached to the back of the tube; a spirally wrapped rope (known as a "vortex shedder"), and a rigid plastic "splitter plate" attached to the back of the tube.

All the techniques achieved some reduction in oscillation, although the flexible plastic and the spirally wrapped rope achieved only minor improvements. The standard hydrodynamic shape performed best, nearly eliminating the oscillation. The rigid splitter plate extending one tube diameter length from the back of the housing achieved nearly the same oscillation reduction. This configuration was used for the subsequent field testing. During these tests, no oscillatory motion of the AOP could be seen.

5.2 Puget Sound Test

During April 1988, a series of tests of AOP operation was conducted in Puget Sound, Washington. The measurements were made northwest of Shilshole Bay, in water depths between 150 and 200 m. The vessel used was the R.V. *Miller*, operated by the Applied Physics Laboratory of the University of Washington. Currents in Puget Sound, primarily tidal, are generally much higher than those in the Arctic. Lower apparent current conditions were obtained by allowing the vessel to drift while the AOP was suspended from the boat.

Relative current velocity profiles were measured during the tests using a Model RD-VM0150 Acoustic Doppler Current Profiler (ADCP) built by RD Instruments of San Diego, California. The depth cell length was set at 4 m with an averaging period of 120 s. With these settings, the ADCP measurements have a short-term accuracy of ± 2 cm/s.

Data were recorded on-board the AOP and also transmitted up the guide wire through an inductive link to a COMPAQ personal computer on the vessel. Pressure, conductivity, and temperature data were recorded at 10-s intervals.

The AOP can be set to reverse direction when reaching the upper and lower pressure thresholds and also after obtaining a specific number of samples since the last reversal. Three deployments, Tests 3, 4, and 5, were conducted on April 8. The AOP settings for each of these trials are provided in Tables 2 through 4.

TABLE 2. Test 3 AOP Settings.

Minimum Depth Threshold	6 m
Maximum Depth Threshold	37 m
Max No. Samples Between Reversals	90
Wing Angle	22 degrees
Buoyancy	+44 gm

TABLE 3. Test 4 AOP Settings.

Minimum Depth Threshold	3 m
Maximum Depth Threshold	137 m
Max No. Samples Between Reversals	600
Wing Angle	
Samples 14 - 171	30 degrees
Samples 383- 574	22 degrees
Buoyancy	
Samples 14 - 171	+44 gm
Samples 383- 574	+27 gm

TABLE 4. Test 5 AOP Settings.

Minimum Depth Threshold	0.5 m
Maximum Depth Threshold	60 m
Max No. Samples Between Reversals	250
Wing Angle	22 degrees
Buoyancy	+27 gm

During the tests, the wind speed ranged from 4 to 12 knots. Over each test period, the vessel drifted approximately 2 km.

Pressure, Temperature and Conductivity Sensor Results

The depth history of the AOP during Test 3 is shown in Figure 6. The initial downward velocity of the AOP was increased as the guide cable was lowered to below the lower threshold depth. Cable payout was completed by scan number 72. At scans 90, 160, and 463, the AOP reached the preset depth thresholds and the wing angle was reversed. The 90-scan time threshold was reached at scans 249 and 339, triggering wing reversal. At scan 507, the AOP was winched to the surface.

The temperature and conductivity data taken during Test 3 are shown in Figures 7 and 8, respectively. The differences between the upcast and downcast measurements made near the surface are due primarily to temporal and spatial variability in the water column. Sensor cell flushing time may also contribute to the differences, especially at the high vertical velocities caused by winching of the guide cable at these points.

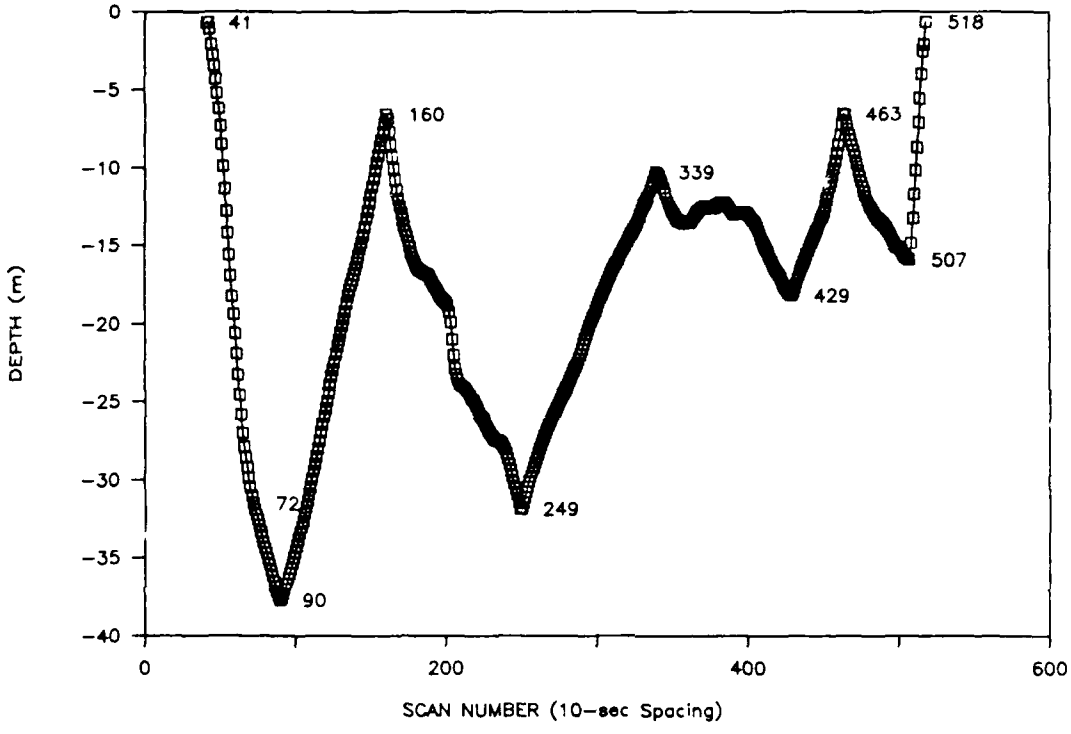

Figure 6. AOP depth profile for Test 3 in Puget Sound. The depth of the AOP at each 10-second scan interval is shown. The numbers in the figure refer to individual scan numbers.

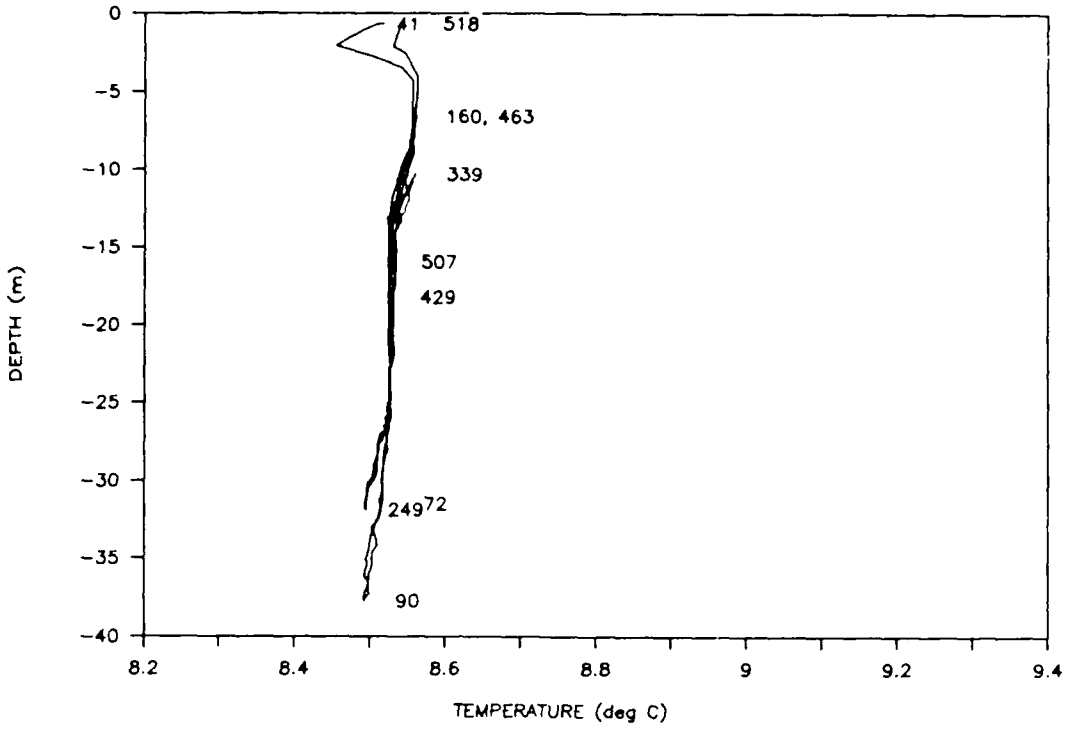

Figure 7. Temperature profiles measured by the AOP during Test 3.

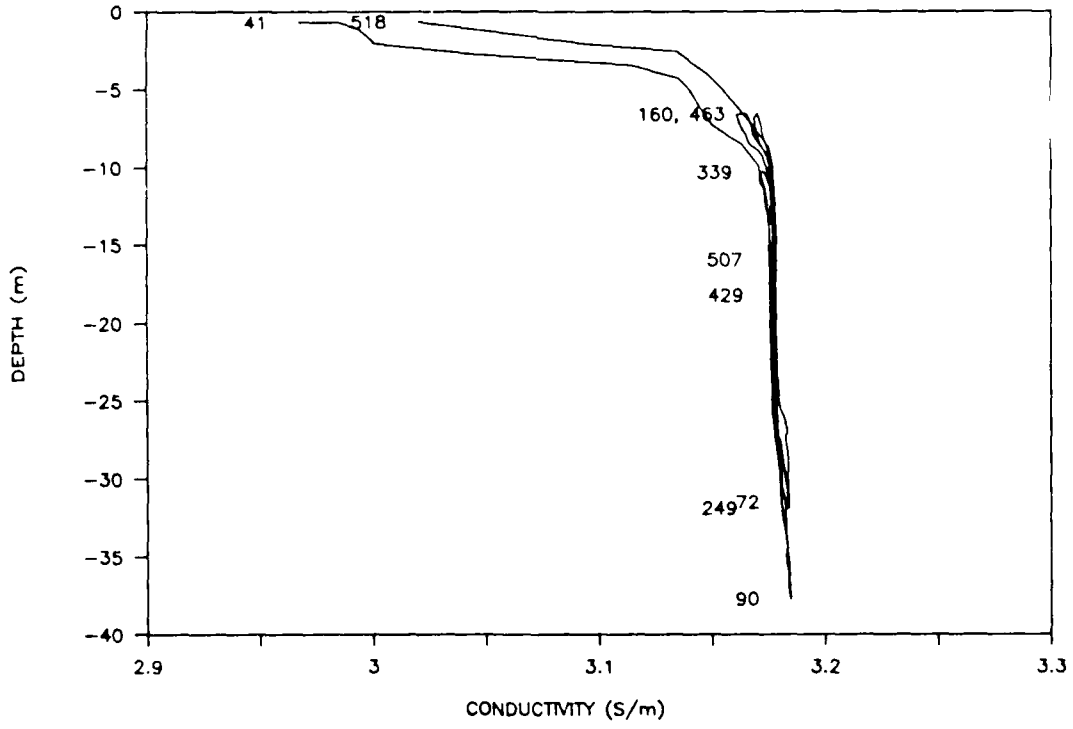

Figure 8. Conductivity profiles measured by the AOP during Test 3.

The depth history of the AOP during Test 4 is shown in Figure 9. Cable payout was completed by scan number 42. At scan 254, the AOP reached the maximum depth threshold and the wing angle was reversed. At scan 484, the wing reversed due to an error in the on-board software. This sent the instrument downward past the maximum threshold, stopping at the weight at the bottom of the cable. At scan 645, the AOP was winched to the surface. The temperature and conductivity data taken during Test 4 are shown in Figures 10 and 11, respectively.

The depth history of the AOP during Test 5 is shown in Figure 12. Cable payout was completed by scan number 32. At scans 64 and 171, the AOP reached the preset depth thresholds and the wing angle was reversed. Wing reversal was triggered at scan 421 upon reaching the maximum sample threshold. The internal software error caused the reversal at scan 485, sending the instrument downward to the bottom weight. At scan 576, the AOP was winched to the surface.

For Test 5, the wing angle was initially set at 30 degrees. The AOP appeared to be binding on the cable from scans 171 to 266. The unit was winched to the surface and the wing angle was changed to 22 degrees for the remainder of the test. The temperature and conductivity data taken during Test 5 are shown in Figures 13 and 14, respectively.

Vertical Velocity

The vertical velocity of the AOP was calculated from the pressure measurements made by the AOP and from the 10-s time interval between samples. For the conditions of Tests 3, 4, and 5, this vertical velocity, averaged over a 10-s period, has an accuracy of 0.4 cm/s.

The vertical velocity of the AOP during Test 3 is shown in Figure 15. The wing of the AOP rotates from the full nose-up to the nose-down configuration in approximately 10 s. From Figure 15, one can see that it took the AOP approximately 2 scan intervals (20 s) to go from full speed in one direction to equilibrium speed in the other direction. Half of this time was taken in rotating the wing.

The vertical velocity of the AOP was compared with the current measurements made with the ADCP to evaluate the utility of the AOP for use as a current measurement device. The AOP data were averaged over time and vertical distance to match the 120-s averaging period and 4-m vertical bin length of the ADCP data. A scatter plot of the results of Test 3 is shown in Figure 16. The plot shows separately the wing nose-up and nose-down data. For this test, the AOP was weighted to be positively buoyant. As a result, as the current speed approached zero, the AOP maintained upward movement.

For the nose-down case, a minimum threshold current speed was necessary to propel the instrument downward. The three data points at near zero vertical velocity occur at a current

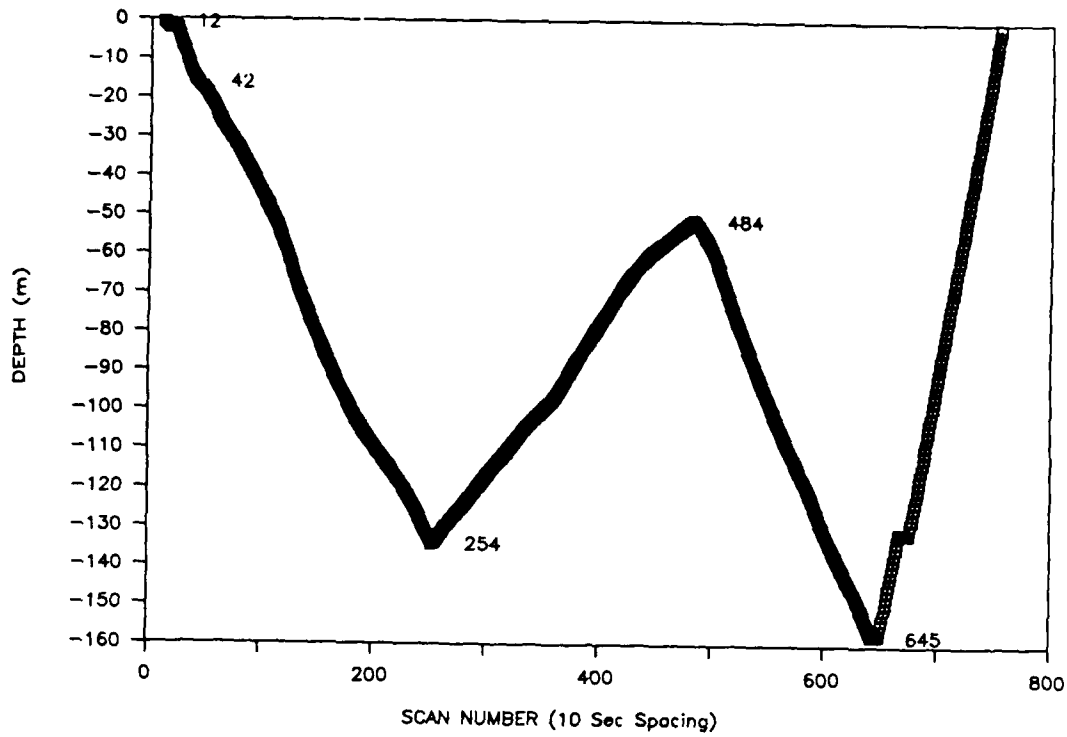

Figure 9. AOP depth profile for Test 4 in Puget Sound. The depth of the AOP at each 10-second scan interval is shown. The numbers in the figure refer to individual scan numbers.

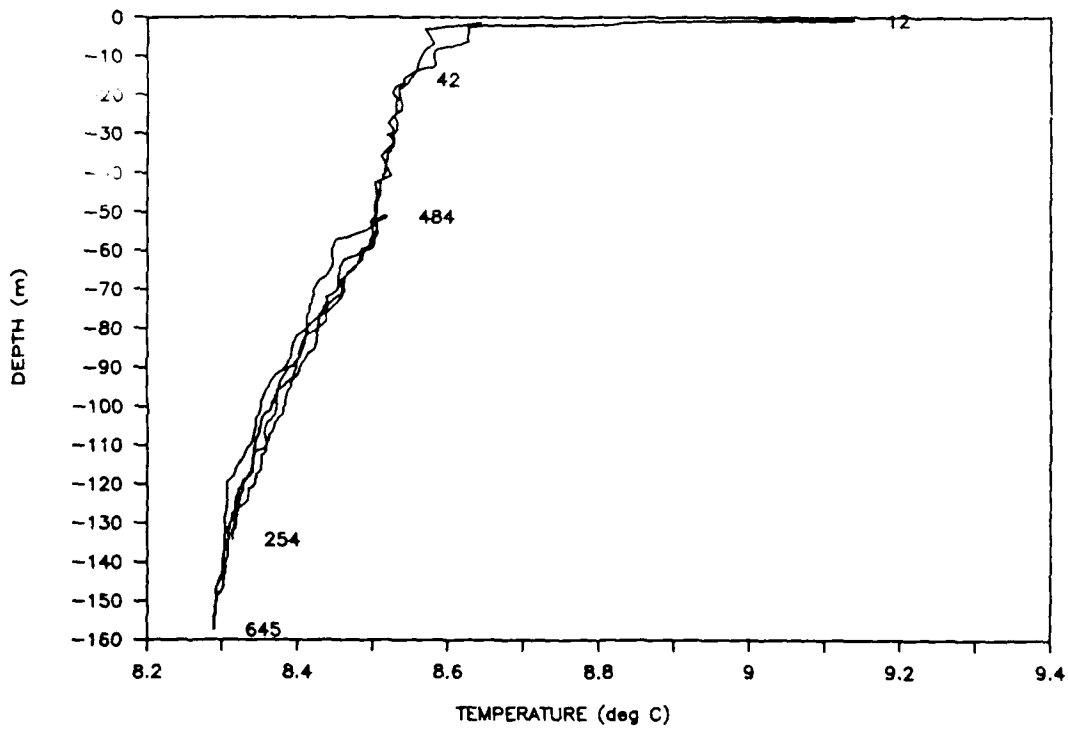

Figure 10. Temperature profiles measured by the AOP during Test 4.

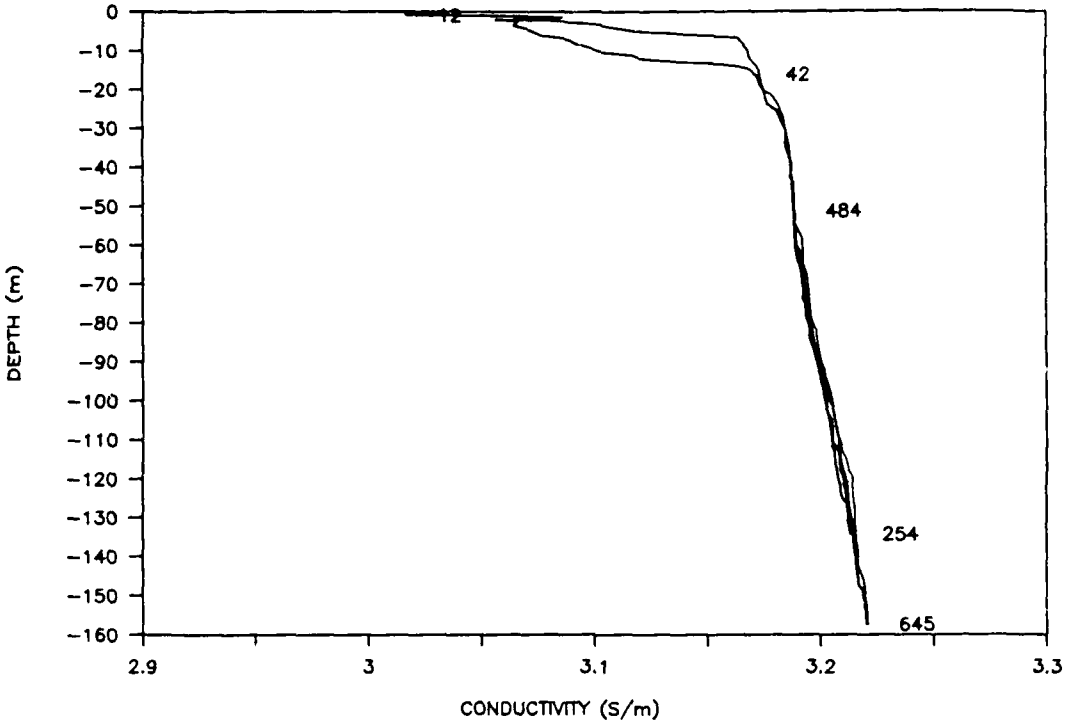

Figure 11. Conductivity profiles measured by the AOP during Test 4.

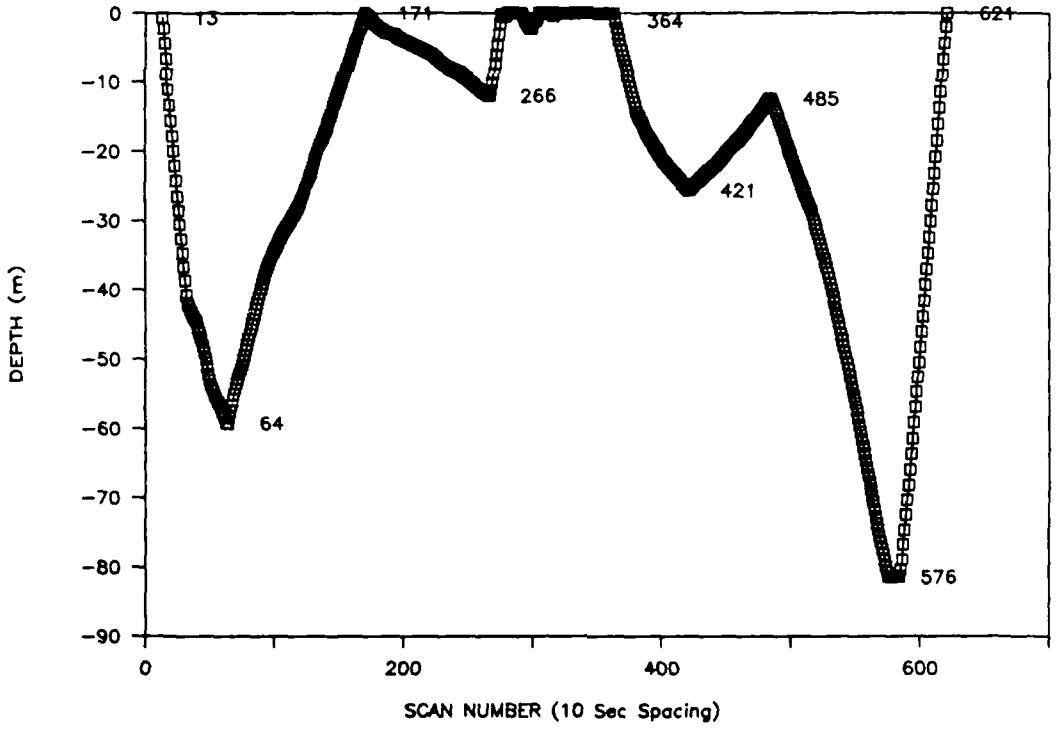

Figure 12. AOP depth profile for Test 5 in Puget Sound. The depth of the AOP at each 10-second scan interval is shown. The numbers in the figure refer to individual scan numbers.

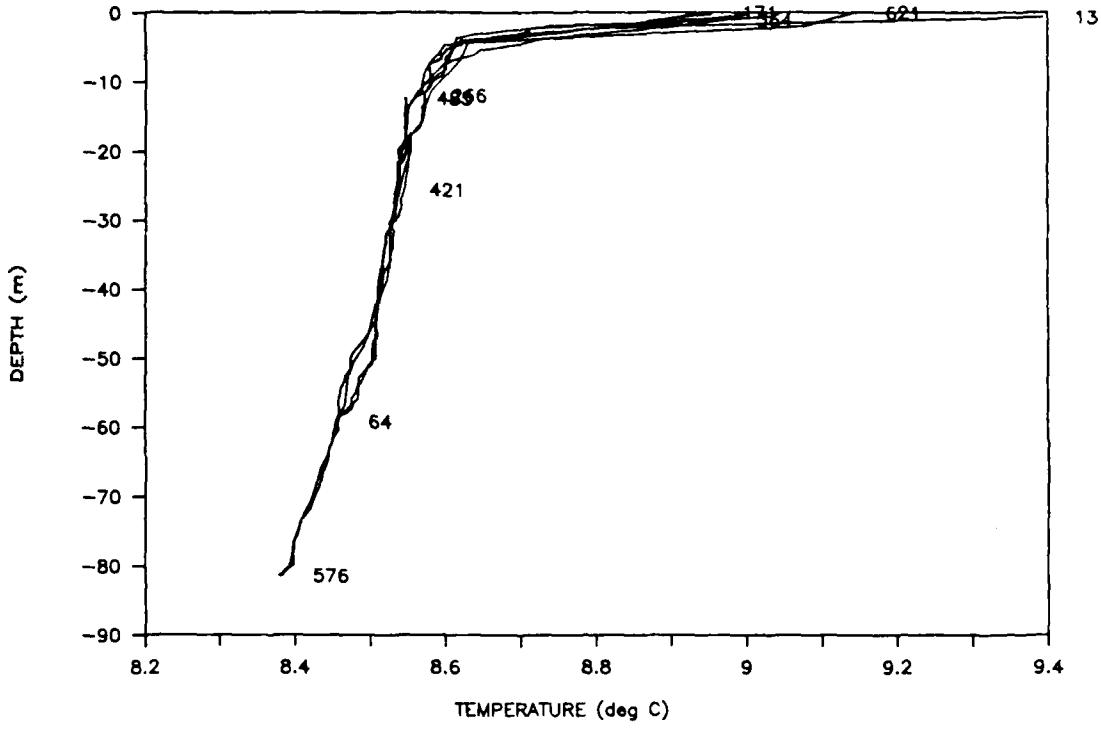

Figure 13. Temperature profiles measured by the AOP during Test 5.

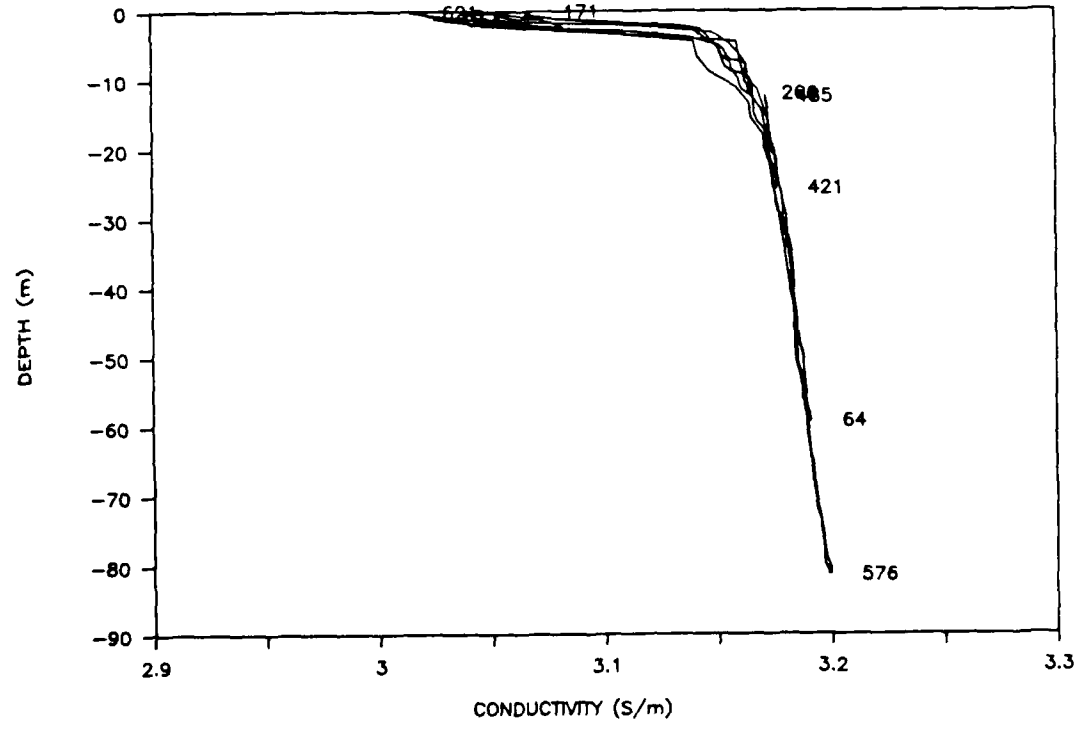

Figure 14. Conductivity profiles measured by the AOP during Test 5.

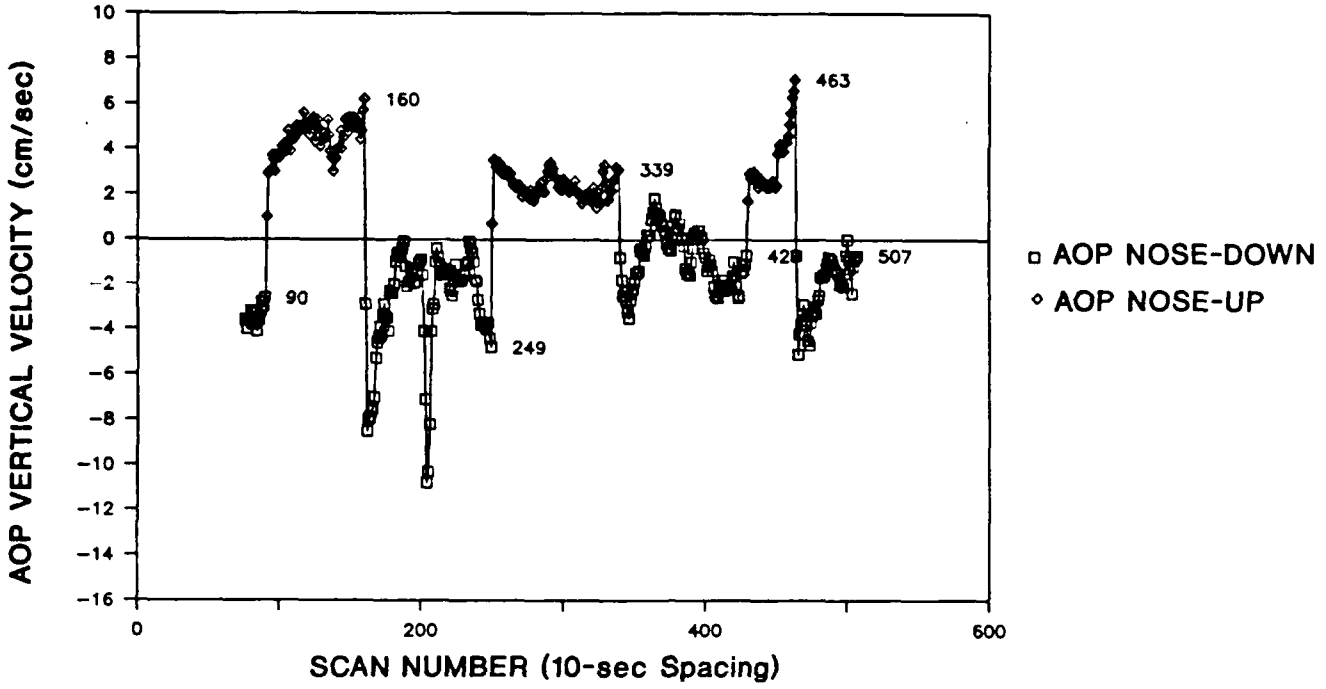

Figure 15. AOP vertical velocity during Test 3 as calculated from pressure sensor measurements from adjacent data points.

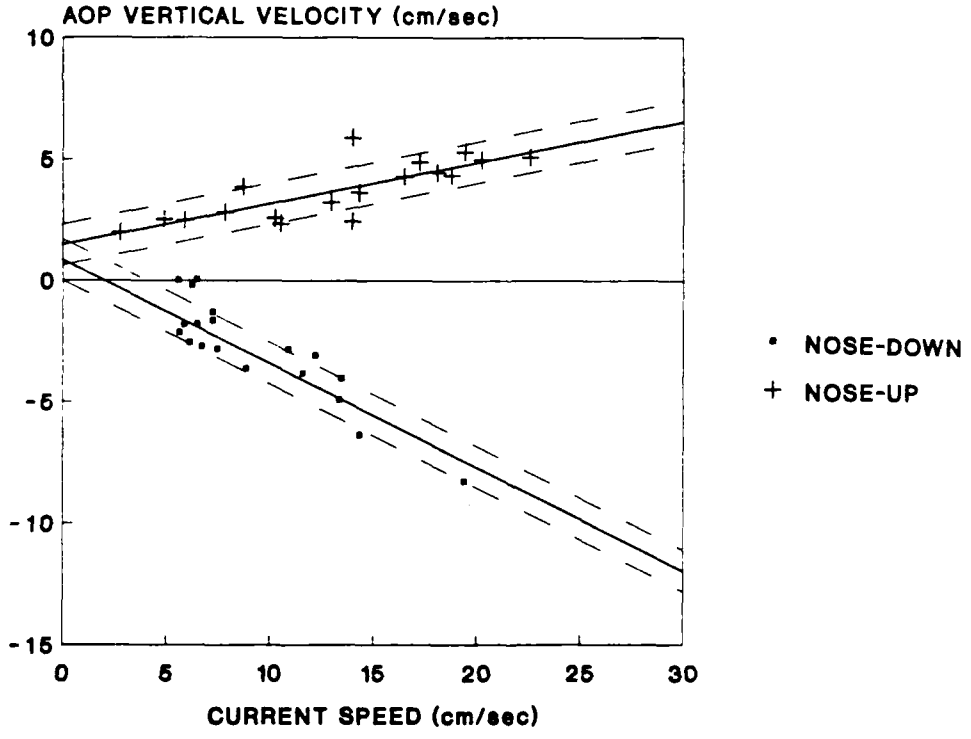

Figure 16. Scatter diagram of AOP vertical velocity versus ADCP current measurements for Test 3. The solid lines are linear regression lines. The dashed lines show the expected error of the ADCP current measurements at the 95-percent confidence interval.

speed of approximately 6 cm/s. The buoyancy of the AOP, at the depth at which these data points were taken, was 44 grams. This weight was calculated from the in situ water density, the displacement of the AOP, and its measured mass. From wind tunnel data [9], the threshold speed of the AOP is calculated to be 6 cm/s, comparing favorably with the value indicated in the field data.

The solid lines in Figure 16 show the least-squares best-fit lines. The line for the nose-down condition was calculated without the three data points near zero vertical velocity. The dashed lines show the expected error of the ADCP current measurements at a 95 percent confidence interval. This indicates that most of the scatter in the plot can be attributed to the error of the ADCP measurements.

The slope of the nose-up regression line is less than that for the nose-down condition. At low current speeds, the slopes are affected by the positive buoyancy of the AOP, but this plays a lesser role at higher current speeds. For current speeds above 10 cm/s, for the nose-up condition, the AOP vertical speed was approximately 26 percent of the current speed as compared to 37 percent for the nose-down condition.

The AOP traveled more readily downward than upward in both the Puget Sound tests and in the Arctic tests (as described in the following section). One possible explanation is that the pitch angle of the wing was biased in the nose-up direction, that is, the nose-up angle was greater than the nose-down angle. After the Arctic tests, the nose-up and nose-down wing angles were measured and were indeed found to be unequal. For the nominal 22-degree case, the nose-up angle measured 19.5 degrees and the nose-down angle measured 24.5 degrees. (For the nominal 30-degree case, the nose-up angle measured 26 degrees and the nose-down, 32 degrees.) From these angles one would expect, for a given current velocity, an approximately 30 percent higher downward velocity than upward. This angular error is likely the cause of the observed up/down speed difference.

Scatter plots of AOP vertical velocity and current speed for Tests 4 and 5 are shown in Figures 17 and 18, respectively. The data taken with wing angles at 22 and 30 degrees (nominal) in Test 5 are shown separately in Figure 18. As would be expected, the AOP vertical velocities for the 30-degree wing angle are higher than for the 22-degree condition.

5.3 Arctic Test

An opportunity became available to conduct a brief, attended test of the AOP in the Arctic. The AOP and ancillary equipment were provided to Dr. James Morison of the Polar Science Center who conducted the Arctic test at no cost to the AOP development program. He tested the unit during a Navy-sponsored ice encampment during March 1988. The test was conducted at a water depth of 500 m in the Lincoln Sea, which is located north of the early

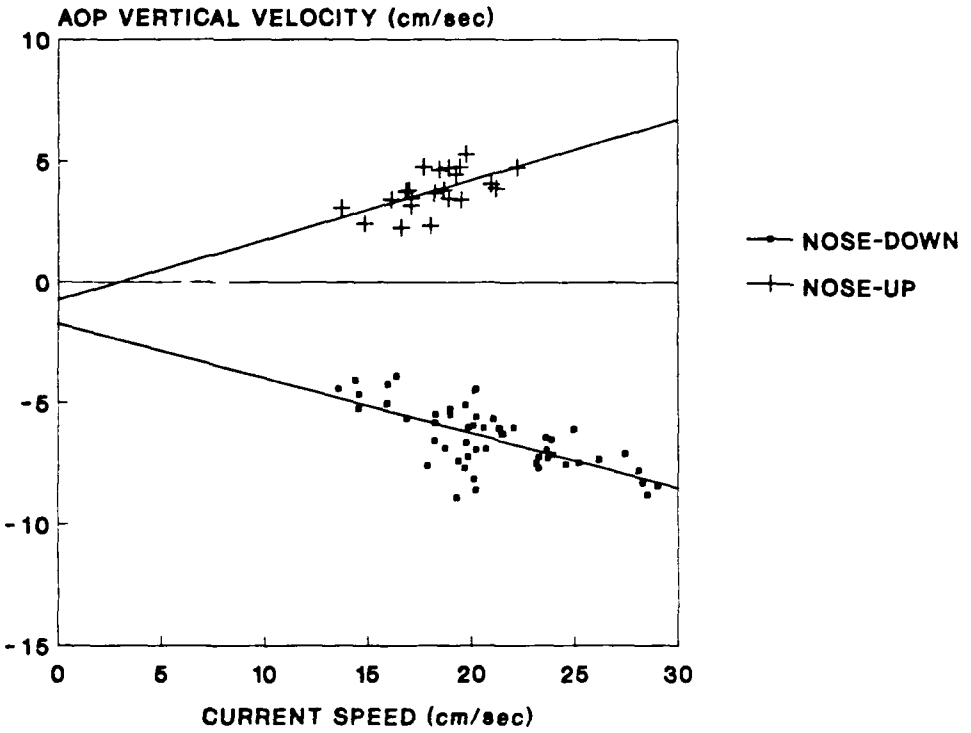

Figure 17. Scatter diagram of AOP vertical velocity versus ADCP current measurements for Test 4. The solid lines are linear regression lines.

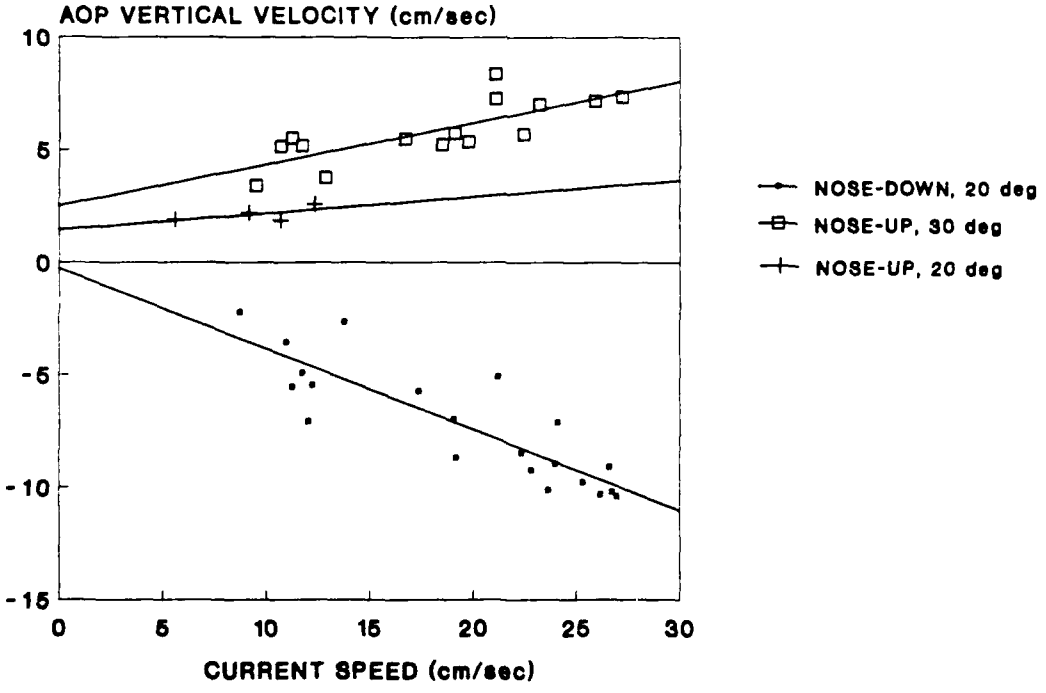

Figure 18. Scatter diagram of AOP vertical velocity versus ADCP current measurements for Test 5. The solid lines are linear regression lines.

warning radar site at Alert, NWT, Canada. The test was conducted on a time-available basis and was not to interfere with the scheduled camp operations.

The short time between the Puget Sound tests and the shipping date for the Arctic did not permit adequate modification and retesting of the unit before shipment. The unplanned nose-down movement at multiples of 485 samples could not be duplicated in the laboratory. Some modifications were made to the electronics in an effort to solve the problem, but the schedule did not allow in-water retesting before shipment. A motor shaft shearing problem was identified in the Puget Sound tests. An interim modification to the shaft and coupling was made but also could not be tested in the water prior to shipment.

Two useful data casts, Jerry 1 and Jerry 3, were made during the Arctic deployment. The specifications for the casts are provided in Tables 5 and 6.

TABLE 5. Jerry 1 Cast Specifications.

Start Date	April 29, 1988
Start Time	23:03
Minimum Depth Threshold	2.0 m
Maximum Depth Threshold	100 m
Max No. of Scans Between Reversals	300
Sampling Frequency	10 s
Wing Angle	22 degrees

TABLE 6. Jerry 3 Cast Specifications.

Start Date	May 1, 1988
Start Time	18:06
Minimum Depth Threshold	3.0 m
Maximum Depth Threshold	120 m
Max No. of Scans Between Reversals	360
Sampling Frequency	10 s
Wing Angle	22 degrees

The depth history during test Jerry 1 is shown in Figure 19. The AOP moved downward slowly to a depth of 39 m. At this point, the maximum number of scans between reversals (300) was reached, and the nose-up command was given internally. The AOP did not rise then but maintained the same depth. At scan 485, an errant command apparently was given and the AOP resumed the descent. At 100 m, the maximum depth threshold, the nose-up command was given but the AOP again did not ascend. At scan 970 (2 x 485) an errant nose-down command was given and the AOP moved downward, past the lower threshold limit, stopping at a depth of 111 m. At this level, little movement was made by the AOP. After 8300 scans it was winched to the surface. At the surface, the drive shaft for the wing rotation was found to be sheared.

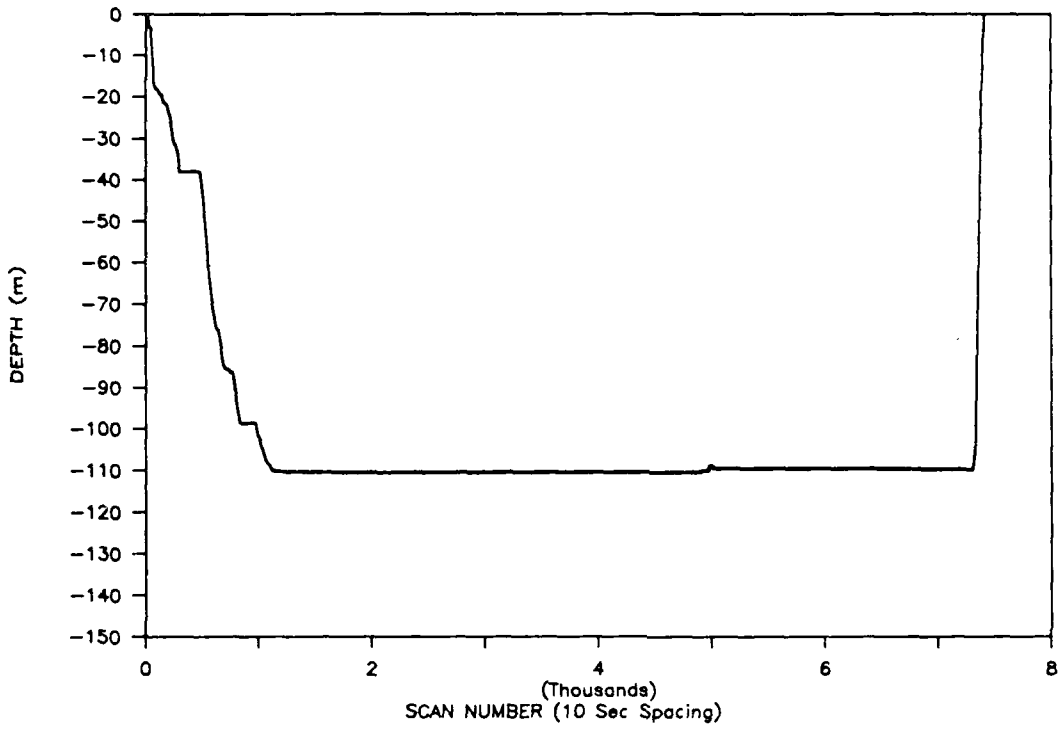

Figure 19. AOP depth profile for Arctic test Jerry 1. **The depth of the AOP at each 10-second scan interval is shown.**

The reason for the lack of upward movement of the AOP is not clear. It was noted in the Puget Sound tests that, in its tested configuration, the AOP moved more readily in a downward direction. It may have been the case that local Arctic currents were sufficient for downward movement but insufficient for upward movement. The drive shaft may have sheared after reaching the maximum depth, thereby neutralizing any further up/down commands. It is also possible that the shaft was sheared while the AOP was winched to the surface.

The temperature and conductivity data gathered during test Jerry 1 are shown in Figures 20 and 21, respectively. The downward vertical velocity of the AOP ranged from less than 1 to 4.2 cm/s. The upward velocity during winching was 14 cm/s. This difference in velocity affected both the temperature and conductivity data. The maximum difference between the up and down casts for each sensor was about 7 ppt. This effect can be seen most clearly in the conductivity data, where the upcast data lagged the earlier data. In the upper layer of near-constant conductivity, the upcast data matched the downcast data at a point near the surface. This effect can be reduced by adding deflectors to increase flow through the sensor cell. It should be noted that the winching velocity to the surface on the upcast was much higher than would be seen in normal AOP Arctic operations. Therefore, the data gathered during the upcast are not representative of normal AOP data.

A field repair was made to the drive shaft, and the AOP was launched for test Jerry 3. The AOP depth history for test Jerry 3 is shown in Figure 22. Here, at a depth of 70 m, the AOP reached the maximum number of scans between reversals (360) where it rotated the wing and motion stopped. At scan 485 the nose rotated downward, and the downward motion resumed until reaching the maximum depth threshold at 120 m. Here vertical motion stopped, perhaps due to low current conditions. Downward motion resumed at a multiple of 485 scans (scan 1940). The downward movement was stopped at a depth of 137 m, the bottom of the cable. Sluggish up/down motion occurred until the end of the record.

Temperature and conductivity profiles gathered during test Jerry 3 are shown in Figures 23 and 24. Both profiles correspond well with the downward profiles of Jerry 1, indicating the differences between the up/down profiles in Jerry 1 were not the result of temporal variation.

The AOP was not reliably and consistently propelled by the currents in the test region. This could be remedied in two simple ways. The first would be to use a greater wing angle, for example using 30 degrees instead of 22 degrees. This, in fact, was the plan for the Arctic test, but a miscommunication with the field team resulted in the 22-degree configuration that was used. The other way would be to increase the size of the wing. This could easily be done for an expendable application, in which the wing could be rolled up and placed through a small hole. In this attended application, the wing size was limited to the size of a hole that could be made using available time and equipment.

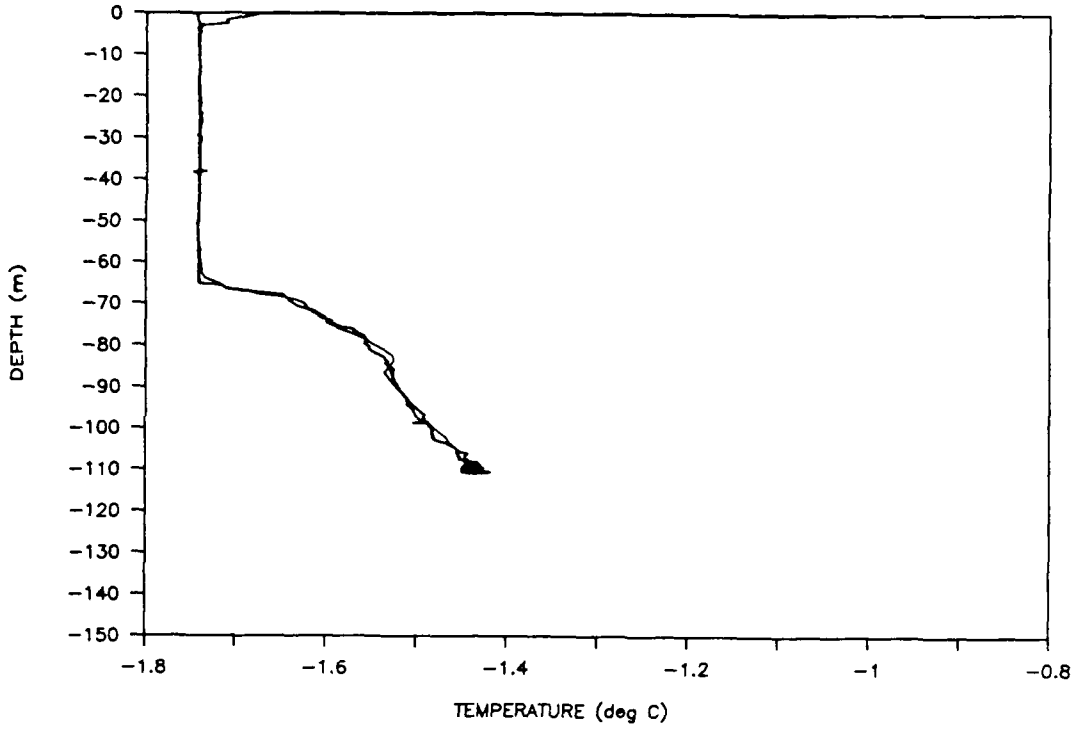

Figure 20. Temperature profiles measured by the AOP during Arctic test Jerry 1.

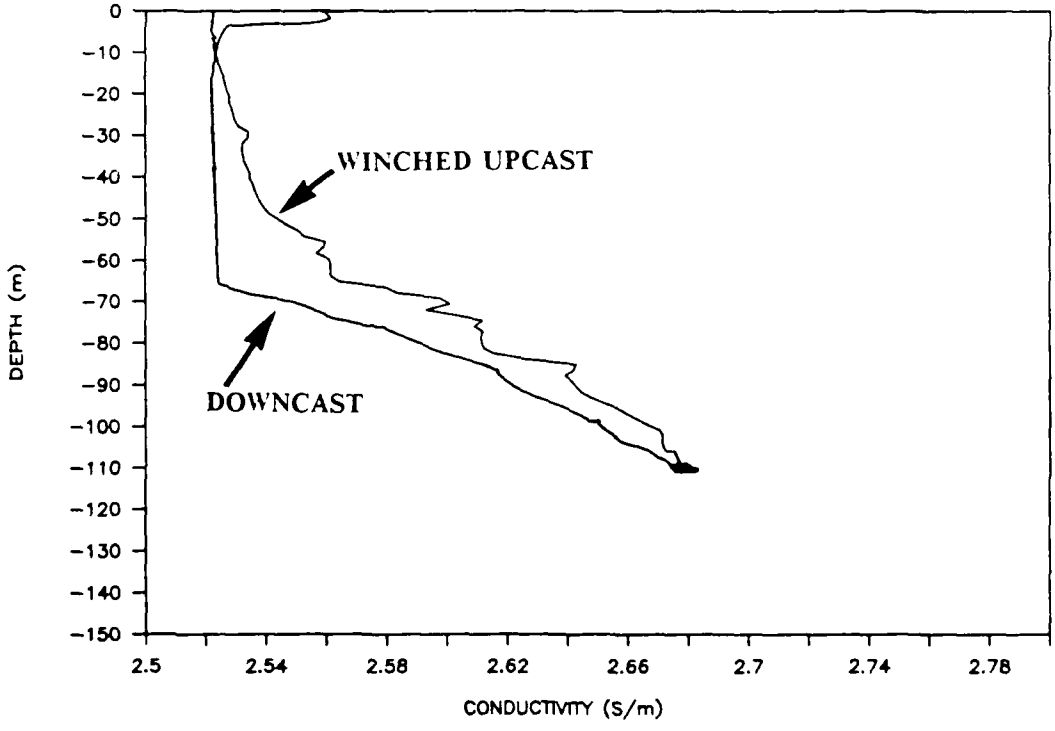

Figure 21. Conductivity profiles measured by the AOP during Arctic test Jerry 1.

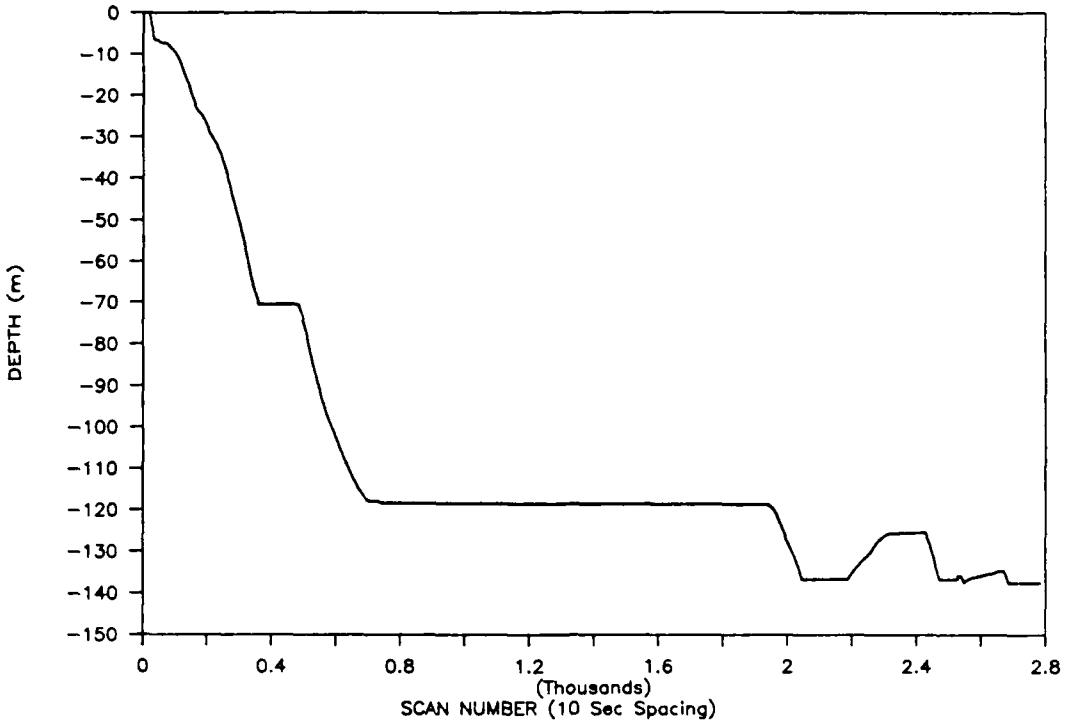

Figure 22. AOP depth profile for Arctic test Jerry 3. The depth of the AOP at each 10-second scan interval is shown.

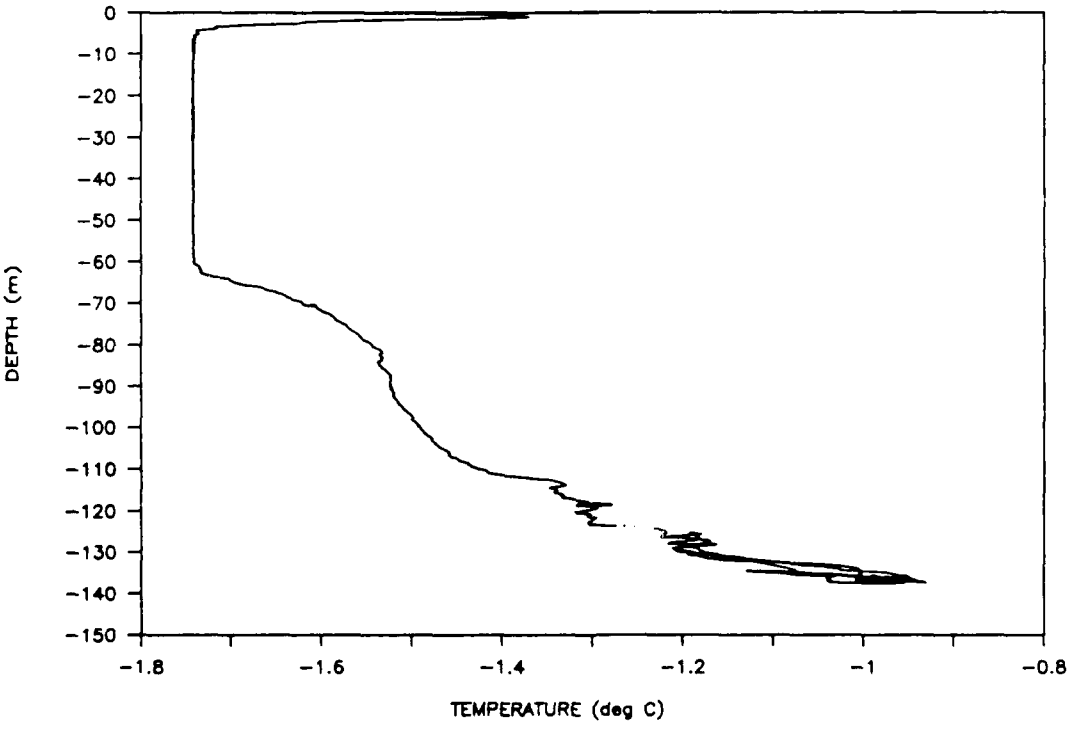

Figure 23. Temperature profiles measured by the AOP during Arctic test Jerry 3.

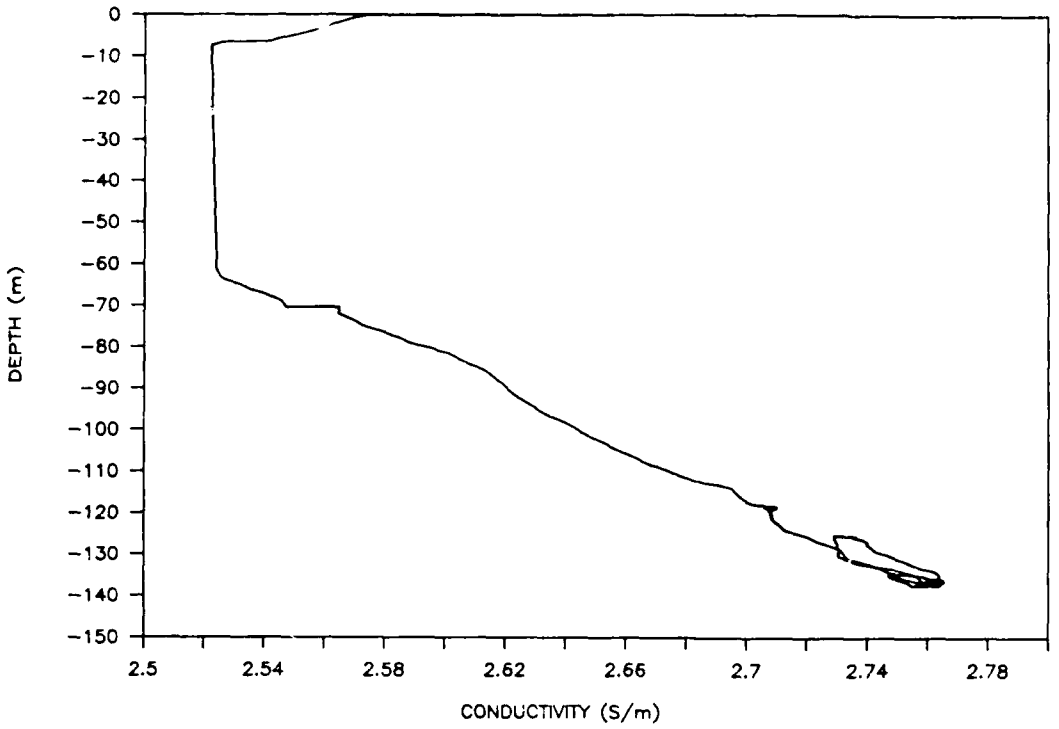

Figure 24. Conductivity profiles measured by the AOP during Arctic test Jerry 3.

5.4 Equipment Modifications and Future Testing

The minor software and mechanical problems identified in the Puget Sound and Arctic testing have been corrected. Under SBIR Phase III (Commercialization) it is planned to retest the AOP in Puget Sound and to conduct an additional Arctic test as a part of a future manned camp program.

6. CONCLUSIONS

The concept of a current-driven profiling instrument has been shown to have good potential for meeting the need for automatic, unattended, long-term ocean profiling. The following general conclusions can be made:

- o A delta wing is more appropriate for the AOP than a rectangular wing. This is because of its high lift performance at low Reynolds numbers and the low span for a given wing area. For Arctic applications, a further advantage is that a thin flat plate can be used, so the wing can be rolled up for through-ice deployment.
- o The most severe test of the hydrofoil profiler concept is in regions of low current velocity, such as the Arctic Ocean. Even for currents as low as 3 cm/s, a profiler of physically reasonable dimensions will be able to produce vertical motion from the currents.
- o Operation at even lower currents can be obtained with a larger hydrofoil area or with less deviation from neutral buoyancy.
- o To minimize deviation from neutral buoyancy, the displaced volume of the profiler should be reduced at depth to compensate for the increased water density. This pressure/buoyancy compensation will improve AOP performance at low current speeds.
- o Preliminary field data indicate that the vertical velocity of the AOP can be used as a measure of current speed.
- o The Autonomous Ocean Profiler will provide greater vertical resolution, over longer periods of time and at lower cost, than existing unattended profiling systems.

REFERENCES

[1] Morison, J., S. Burke, H. Steltner, and R. Anderson, "SALARGOS Temperature-Conductivity Buoys," *Oceans*, pp. 1255-1260, September 1982.

[2] Van Leer, J. C., "An Automatic Oceanographic Profiling Instrument," *ISA ASI* 7626B, pp. 489-500, 1976.

[3] Eriksen, C. C., J. M. Dahlen, and J. T. Shillingford, Jr., "An Upper Ocean Moored Current and Density Profiler Applied to Winter Conditions Near Bermuda," *Journal of Geophysical Research*, Vol. 87, No. C10, pp. 7879-7902, September 1982.

[4] Katz, E. J., and R. T. Nowak, "A Towing System for a Sensing Package: Experience and Plans," *Journal of Marine Research*, Vol. 31, pp. 63-76, 1973.

[5] Morison, J. H., and J. D. Smith, "Seasonal Variations in the Upper Arctic Ocean as Observed at T-3," *Geophysical Research Letters*, Vol. 8, No. 7, pp. 753-756, 1981.

[6] Coachman, L. K., and K. Aagaard, "Physical Oceanography of Arctic and Subarctic Seas," in *Marine Geology and Oceanography of the Arctic Seas*, Y. Herman, editor, New York, Springer-Verlag, 1974, pp. 1-72.

[7] Wentz, W. H. Jr., "Wind Tunnel Investigations of Vortex Breakdown on Slender Sharp-Edged Wings," NASA CR-98737, November 1968.

[8] Echert, D. C., E. W. Geller, D. J. Hanzlick, and J. H. Morison, "A Hydrofoil Instrument Platform for Obtaining Profiles of Ocean Properties," Flow Research Report No. 361, Prepared for the Office of Naval Research under Contract No. N00014-85-C-0676, 1986.

[9] Lawford, J. A., and A. R. Beauchamp, "Low Speed Wind Tunnel Measurements on a Thin Sharp-Edged Delta Wing with 70 Degree Leading Edge Sweep, with Particular Reference to the Position of Leading-Edge Vortex Breakdown," A.R.C.R.&M. No. 338, November 1961.

APPENDIX: AOP DESIGN DETAILS

This appendix provides additional details of the AOP system design. Included are sections on alternative design configurations, lifting requirements and wing sizing, and design of the guide cable bottom weight.

A.1 ALTERNATIVE DESIGN CONFIGURATIONS

Three different AOP design concepts were developed. Each is based on a different assessment of the amount of stored energy available or needed onboard to effect the large number of vertical motion reversals that have to be made during one year of deployment. In the order presented, the designs require increasing onboard energy storage. They were developed in that order as those requirements were more accurately assessed and as new information for design was obtained and as new design ideas were formulated.

The first design requires no onboard energy. The work required to operate the canard elevator for turnaround is extracted from the environment and for that reason the design is "passive". The other two designs are "active". They use energy from an onboard source to effect the turnaround. The first of these active designs requires energy to rotate a canard and differs from the passive design in that this energy is supplied by an electric motor instead of by the ocean current. The second of the active designs uses an electric motor to rotate the entire wing directly and thus dispenses with the canard. It requires the largest amount of onboard energy storage and was originally thought not to be feasible because of these energy storage requirements.

Two Designs Using a Canard

The first design is shown in Figure A-1. The payload housing is on the wing. A canard is used to supply the pitching moment for rotating the wing to reverse the direction of travel along the vertical cable. The canard is rotated using energy extracted from collision with bumpers at the top and bottom of the cable. A mechanical linkage is used to transmit the bumper collision force to the canard to effect rotation. The rotated canard supplies a hydrodynamic moment to rotate the wing. The design is passive in that no energy from an onboard source is used to drive the rotation. Stops are used to limit the pitch angle to ± 30 degrees. The pitch axis is located behind the aerodynamic center so that the system is unstable in pitch and is driven against one or the other of the stops depending upon the position of the canard. Likewise the canard is unstable in rotation about its hinge so that it too is driven against a stop, in this case one supplied by the cable in the linkage system between the bumper and the canard.

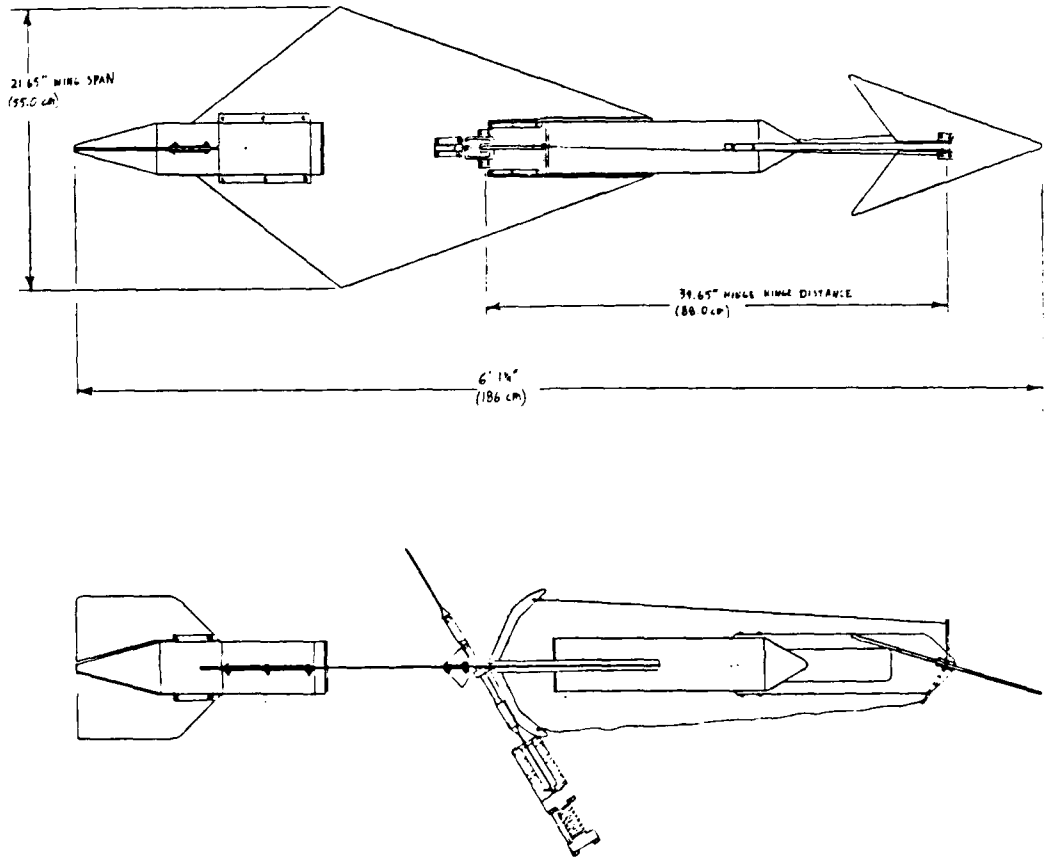

Figure A-1. AOP Design Concept Number 1. The payload is mounted on the wing and a passive pitch control is used.

In Figure A-1 the hydrofoil is shown just as it contacts the lower bumper which is about to actuate the mechanism to rotate the canard to an upward position. Note that the lower control cable is slack. The upper cable is about to pull the canard in an upward rotation about its hinge. As soon as the canard experiences a change of angle of attack from negative to positive it will also experience an upward moment about its hinge due to hydrodynamic forces. This occurs because the hinge is behind the center of pressure of the canard. The upward hydrodynamic force that the canard experiences when it gets to a positive angle of attack will rotate the wing upward until it hits a stop. The wing will then generate an upward force and the system will move in the upward direction to complete the turnaround maneuver.

The second design is shown in Figure A-2. It differs from the first design in that an electric motor is used to rotate the canard. The motor is buried in the canard with its axle serving as the canard hinge. This motor requires additional hardware, a microprocessor for control and batteries for power. By programming the microprocessor to limit vertical traverses to several times a day with parking at the top, the number of turnarounds that occur over the one year deployment period is drastically reduced from that of Design No. 1, and it was determined that the battery requirements for driving the canard for this reduced number of cycles was acceptable.

A fundamental problem exists for Designs No. 1 and 2 which results from the inability of the canard to supply a pitching moment that will counteract the couple that occurs when the oppositely directed and nearly equal gravity and buoyancy forces are not precisely aligned. The lines of action of these two forces go through the center of mass and the center of volume, respectively. This problem is most serious at the minimum current condition. The design is based on a very small deviation from neutral buoyancy. The weight in water is assumed not to exceed one thousandth of the weight, and the wing is sized to provide a lift at the minimum current condition to balance this extremely small weight in water. Thus the hydrodynamic forces at minimum current are of the order of one thousandth of the buoyancy and gravity forces, and it is not surprising that misalignment of the latter two by only a fraction of a millimeter will produce a couple that can not be counteracted by hydrodynamic pitch control, that is by the canard.

Two solutions were devised for this problem. One is to use a ballast weight that can be moved longitudinally with precision using a screw thread. Adjustment to its proper position that gives alignment of the center of gravity (CG) and the center of buoyancy (CB) to within the needed tolerance is accomplished by a difficult laboratory procedure. The hydrofoil is submerged in water in a horizontal position and released. The subsequent angular velocity in pitch is a measure of the misalignment of the CG and CB. The ballast weight position is adjusted until this pitch velocity is sufficiently small. Each unit manufactured would require

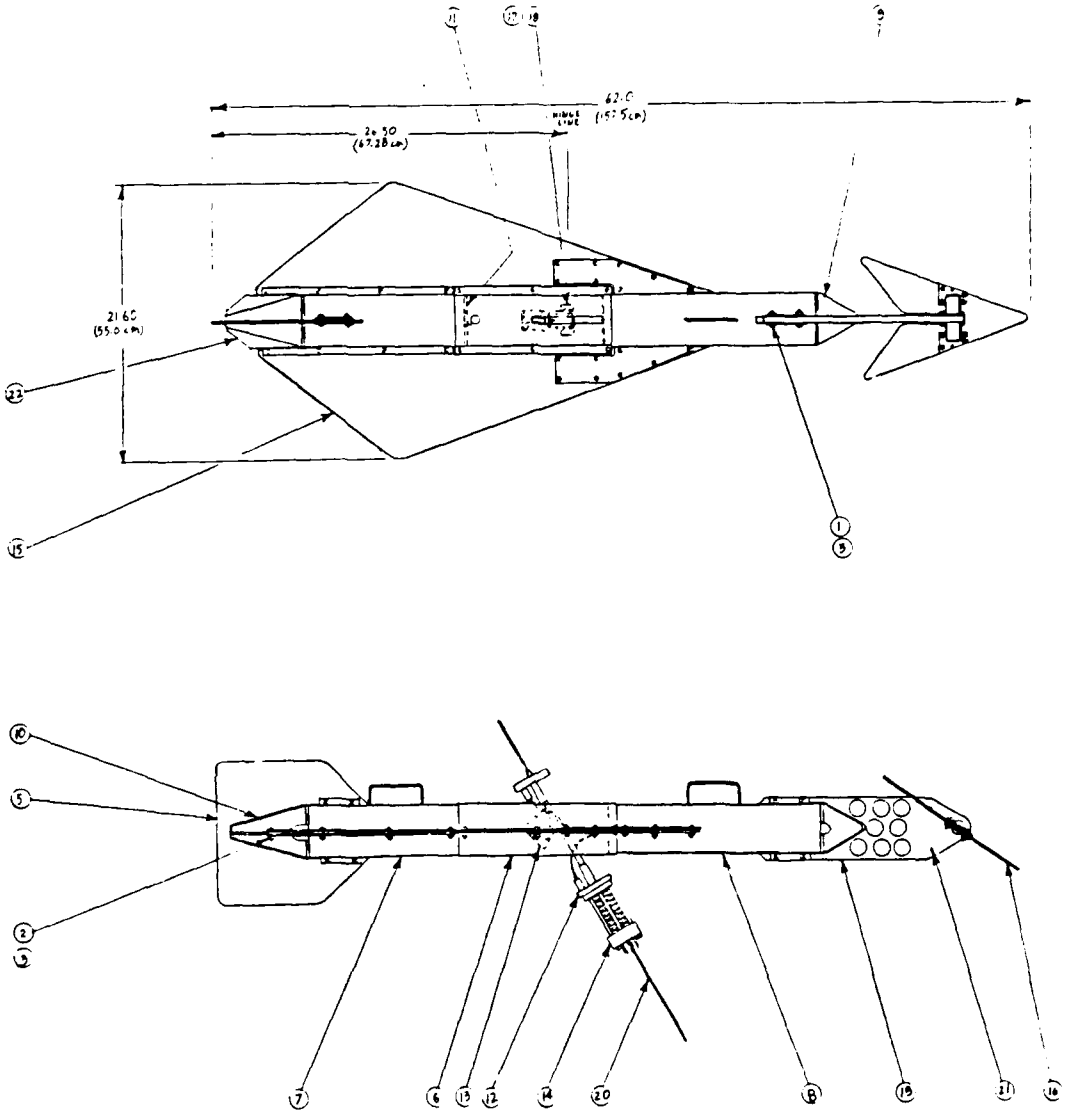

Figure A-2. AOP Design Concept Number 2. The payload is mounted on the wing and active pitch control with a canard is used.

this laboratory "tuning" before being used in the field. The critical pitch velocity not to be exceeded in this tuning procedure would have to be determined by a careful calibration test on the prototype. Besides the expense of tuning each unit produced, this solution has the additional disadvantage of not allowing very much biofouling during deployment. Accretions may upset the critical balance obtained in the laboratory. This may not be a problem for deployment in the Arctic.

The second solution does not have the two disadvantages just mentioned. A small ballast weight is driven longitudinally by an electric motor at the same time that the canard is actuated. The requirement for ballast size and throw distance is that the pitch moment due to CG and CB misalignment change sign when the ballast is moved by the electric motor. The same arguments used above to indicate how critical is this misalignment can be used to show that the required ballast size and excursion is small and that the added energy requirements for this solution are acceptable. The disadvantage is the need for an additional motor or linkages for drive from the primary motor and the additional battery requirements. The canard is still required at high currents to counteract the hydrodynamic moment due to misalignment of the center of pressure with the wing hinge line.

There is another drawback associated with the need for precise management of the centers of mass and volume. Any change in payload (e.g., batteries or instrumentation) requires a redesign for payload placement to maintain CG and CB alignment. The second solution above would allow some tolerance to payload change if the moveable ballast throw distance is large.

The Prototype Design

The third design is shown in Figure A-3. Whereas the first two designs placed everything on the rotating wing, the third design offloads everything from the wing onto a package which is pushed by the wing up and down the vertical cable to which it is attached. Thus any change in the payload does not require extensive redesign to maintain proper balance of the rotating part. In fact no change is required if the payload housing is made sufficiently large to accommodate expected payload changes. Also, since the driving force for wing rotation for this design is the electric motor, the requirement for aligning the center of mass and center of volume with extreme precision is gone. In fact alignment itself is not needed. It is only necessary that the line of action of the wing's weight in water be approximately aligned with the wing hinge.

The rotation of the main wing rather requires more work against hydrodynamic forces than rotating a canard since the wing is a much larger surface, but it was demonstrated that the battery requirements are feasible if appropriate design features are incorporated. Wind tunnel tests [A1] show that a 70 degree simple delta wing has a fixed center of pressure (CP) for all

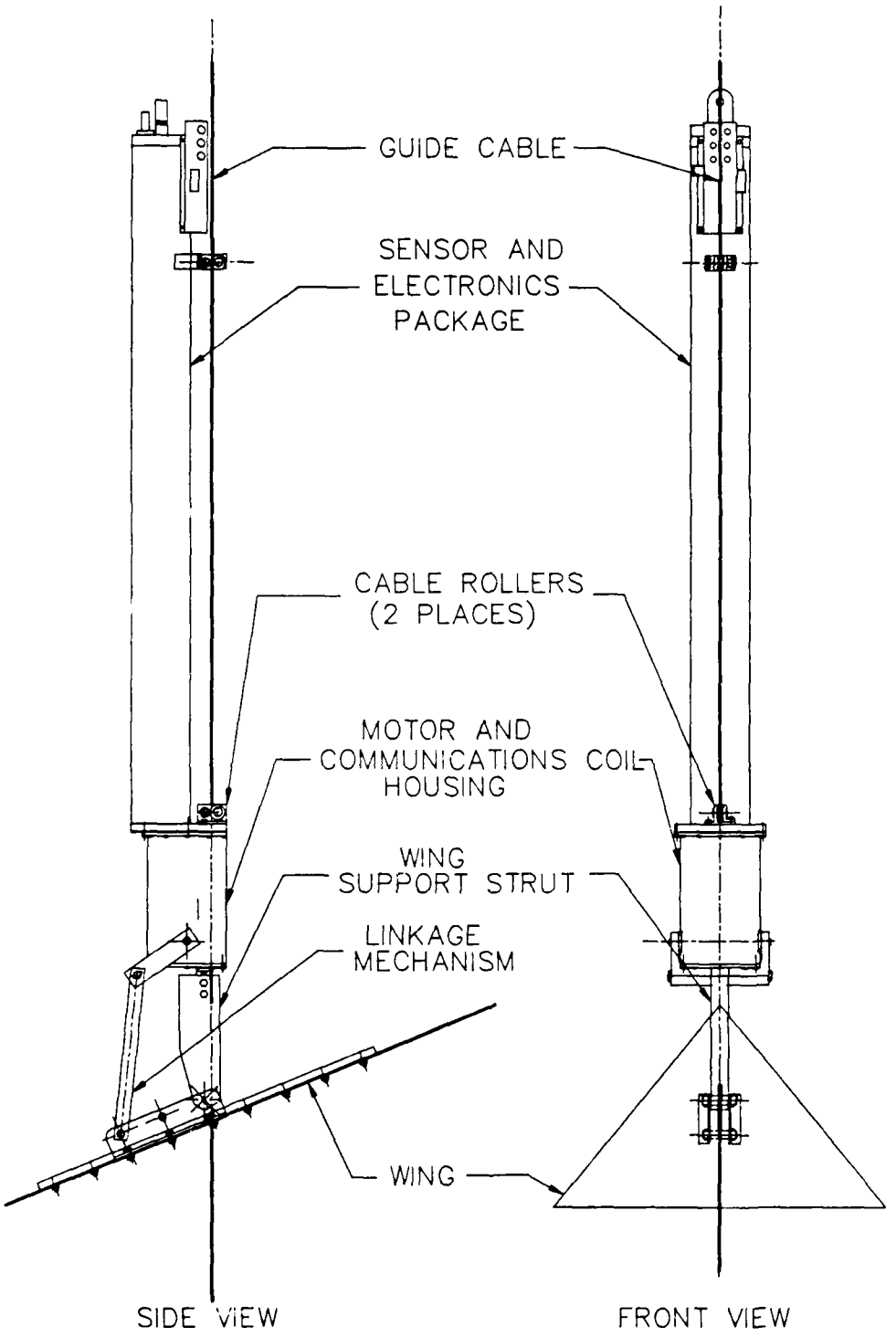

Figure A-3. **AOP Design Concept Number 3. Prototype design with active pitch control by direct drive of the wing and with the payload not attached directly to the wing.**

angles of attack below 22 degrees. Thus if the hinge line is placed at this center of pressure location there will be no hydrodynamic moment for the electric motor to overcome (except for damping due to angular velocity) provided the wing stops are placed at ±22 degrees. At greater angles, the center of pressure moves off of the hinge line requiring additional electrical power to effect the rotation.

The wind tunnel tests are for an isolated wing. With the payload housing moved off of the wing as shown in Figure A-3, this condition will be met approximately. The presence of an object near the wing will cause some shift in the CP but this will be small for the standoff distance of the design shown in Figure A-3.

In order to reduce hydrodynamic interference for the reasons given above and in order to facilitate fold-up for deployment through a small hole in the ice, the hinge line is placed above the wing as shown in Figure A-3. This shift away from the CP will not significantly alter the hydrodynamic moment about the axis if the shift is normal to the wing, since the wind tunnel data indicates that the resultant hydrodynamic force on the wing is nearly normal to the wing at all angles of attack. This is not unexpected since the wing is a flat plate and the predominating force is due to the pressure distribution which is normal to the plate. The surface shear stress felt by the wing (i.e. the skin friction) will produce a small force which will indeed cause a moment as the axis is offset above the wing, but the wind tunnel tests indicate that this moment is tolerable.

Another small moment is incurred by offsetting the hinge. It is produced by the buoyancy and gravity forces on the wing which do not cancel since the average wing density does not match the water density. This discrepancy could be eliminated by using a buoyancy element on the wing (e.g., a small glass buoyancy ball), but it was determined that the moment penalty incurred by having a wing with a positive weight in water could be tolerated. This moment varies with angle of attack, and to minimize the excursion, the center of volume and the center of mass of the wing are set so that the line of action of the weight in water passes close to the hinge when the wing is at zero pitch.

A.2 LIFTING REQUIREMENTS AND WING SIZING

Since it is not possible to maintain neutral buoyancy over the entire operating cycle for the profiler, it is necessary to generate lift to counteract its weight in water. Although the deviation from neutral buoyancy can be made very small, the lifting capability is a major design problem, since the currents available to generate lift are extremely small. Of course, a wing can always be made large enough to generate a specified lift at a specified current speed. A major goal for the design is to minimize the wing size.

If the platform is neutrally buoyant, then it can generate sufficient lift for traversing no matter how small the wing and how low the current. However, neutral buoyancy is not possible at all times, because of spatial and temporal variations in water density and changes in profiler density from water absorption during long-term deployment. We explain in the following how the maximum deviation from neutral buoyancy during the annual operating cycle dictates the size of the wing, and we discuss features or characteristics of the platform that can be used to minimize its size. First, however, we discuss the spatial and temporal water density variation for the profiler operating environment and the variation of the profiler density that occurs with the use of buoyancy compensation.

The density of the Arctic Ocean varies with depth and with time over the annual operating cycle for the platform. As a design specification, we take the envelope of this variation to be that shown in Figure A-4. Near the surface, the density gradient is large as is the temporal excursion. It is in this mixing and melt region that water conditions vary the most.

The density of the profiler is approximately constant unless a buoyancy compensator is used. With the use of a buoyancy compensator, the volume of the profiler and, hence, its density can be set at any values at the top and bottom of the excursion. With proper compensator design, the variation of platform density can be made nearly linear with depth. Appropriate choices for platform density are shown in Figures A-5(a) and A-5(b) for the uncompensated and compensated designs. The objective is to minimize the maximum difference between platform density and water density.

The size of the wing is dictated by operation at the threshold current and at the maximum deviation of water density from platform density. For this operating condition, the wing lifting capability is minimum and the weight in water is maximum (in magnitude). For the following derivations, the subscript max implies maximum value. At the threshold condition, the angle of attack of the wing is its pitch angle (there is no vertical velocity). By definition of the lift coefficient, the lift at the critical operating condition is therefore

$$L = C_{Lmax} \tfrac{1}{2} \rho_w U_{min}^2 S \qquad (A.1)$$

where

C_{Lmax} = lift coefficient at an angle of attack equal to the pitch stop angle
ρ_w = mass density of the water
U_{min} = minimum current speed
S = wing area

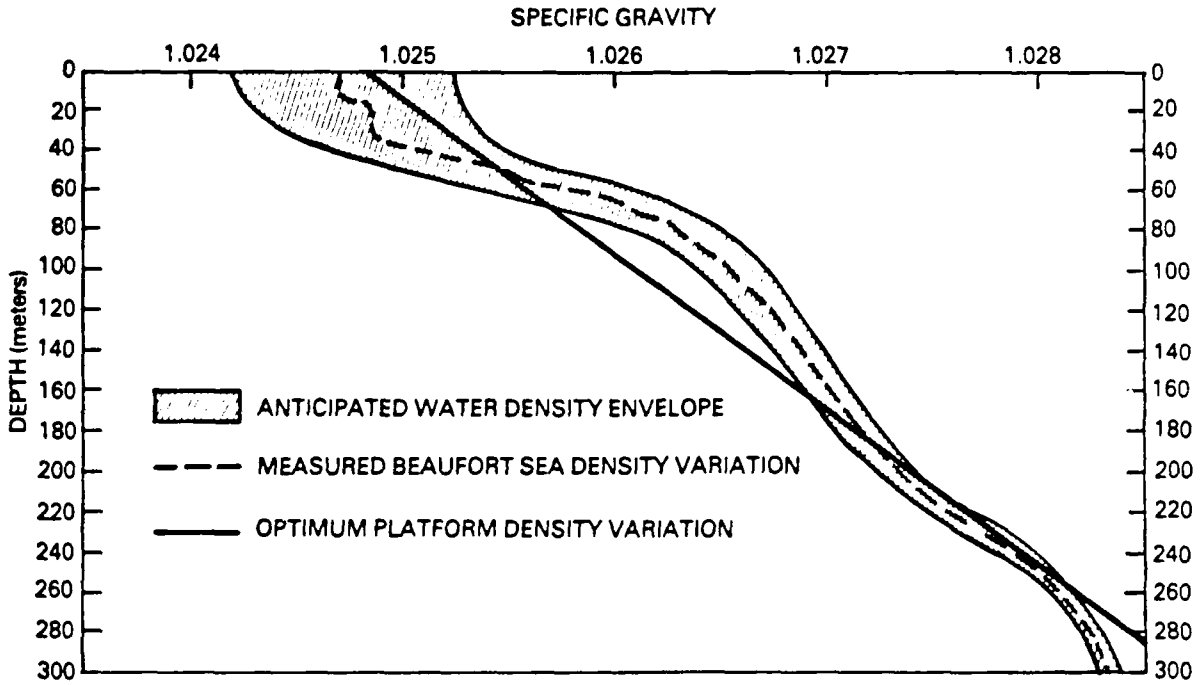

Figure A-4. Arctic seawater density envelope. **The optimum linear density variation of the AOP with depth is shown.**

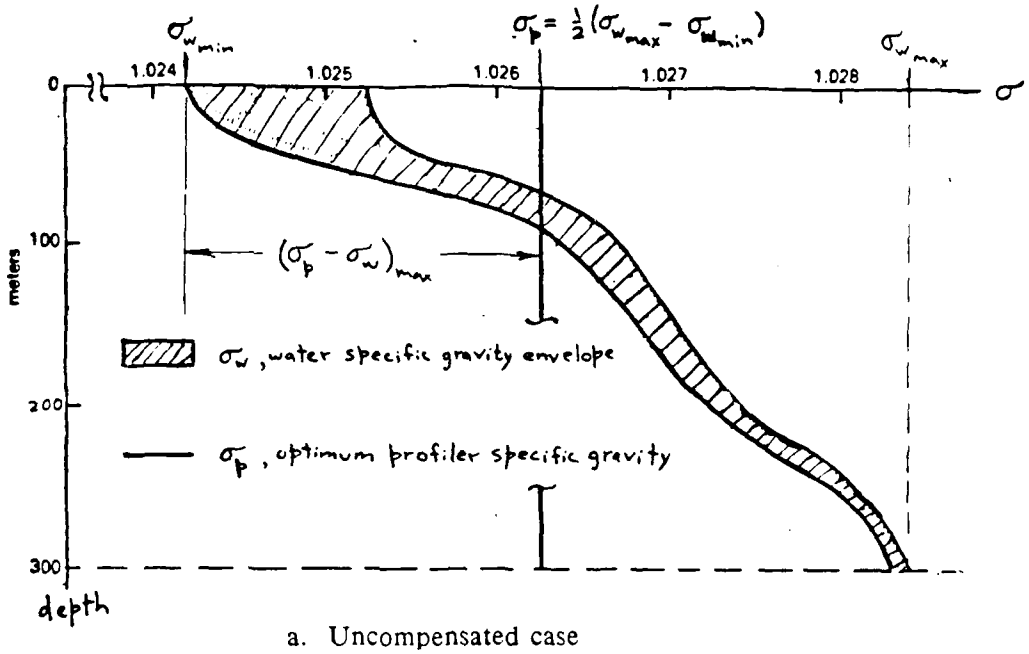

a. Uncompensated case

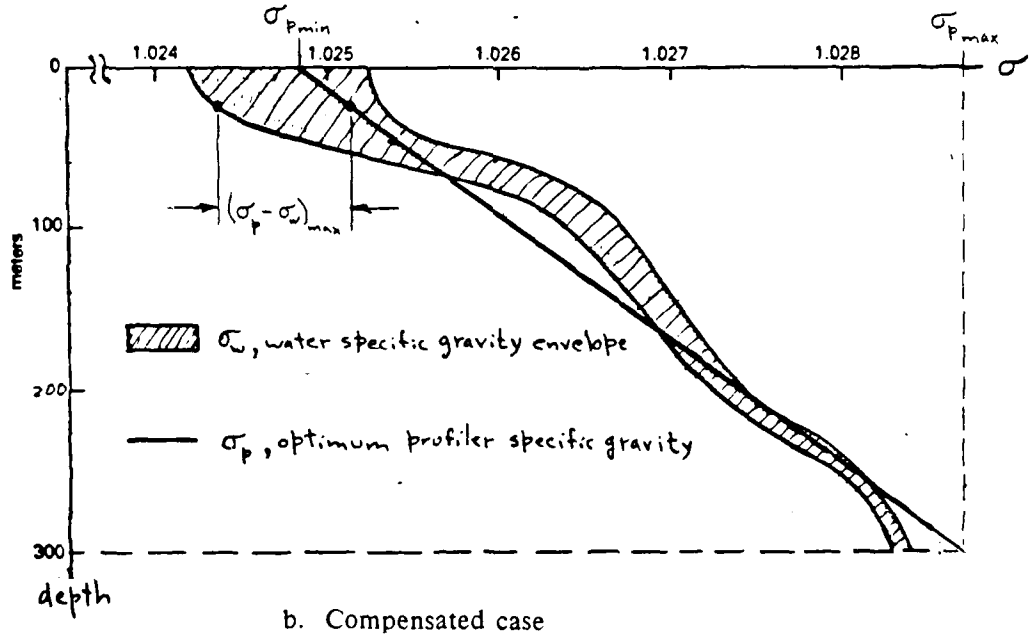

b. Compensated case

Figure A-5. Optimum profiler density. **Figure A-5a is for the non-pressure-compensated case and Figure A-5b is for a system using pressure-compensation.**

At the critical condition, the lift counteracts the weight in water and the cable friction so that

$$L = W'_{max} + \mu D = g(\rho_p - \rho_w)_{max} H + (\mu D/L)L \qquad (A.2)$$

$$\approx g(\rho_p - \rho_w)_{max} H = g \rho_o H(\sigma_p - \sigma_w)_{max}$$

where

W'	=	profiler weight in water
D	=	profiler drag
μ	=	coefficient of cable friction
ρ_p	=	mass density of the profiler
ρ_o	=	reference mass density for specific gravity
σ_w	=	specific gravity of water
σ_p	=	specific gravity of the profiler
H	=	volume of water displaced by the profiler
g	=	gravitational acceleration

The deletion of the cable friction in Equation (A.2) follows from the fact that

$$\mu D/L << 1$$

Combining the preceding equations gives the wing area needed for a prescribed threshold velocity:

$$S \approx \frac{2g H}{C_{Lmax} U_{min}^2} \frac{\rho_o}{\rho_w} (\sigma_p - \sigma_w)_{max} \qquad (A.3)$$

$$\approx \frac{2g H}{C_{Lmax} U_{min}^2} (\sigma_p - \sigma_w)$$

or, conversely, the threshold velocity for a prescribed wing area:

$$U_{min}^2 \approx \frac{2g H}{C_{Lmax} S} (\sigma_p - \sigma_w)_{max} \qquad (A.4)$$

It is interesting to note this replacement that can be made in the preceding equations:

$$\sigma_p - \sigma_w \approx W'/W$$

where W is the profiler weight in air. According to Equation (A.3), to minimize S, we need to minimize the maximum difference between the water and platform densities and also to minimize the platform volume.

The wing size and total volume of water displaced for the initial prototype are

$$S = 2902 \text{ cm}^2$$
$$H = 10{,}000 \text{ cm}^3$$

We assume, as indicated in Figure A-5, that

$$(\sigma_p - \sigma_w)_{max} = 0.2 \text{ percent for no buoyancy compensation, and}$$
$$= 0.1 \text{ percent for buoyancy compensation}$$

From wind tunnel data reported by Lawford and Beauchamp [A1], the lift coefficient at a 22-degree angle of attack (the condition at minimum current operation) is

$$C_{Lmax} = 1.0$$

Using the above values, the minimum current speed is calculated from Equation (A.4) to be

$$U_{min} = 3.8 \text{ cm/s with no buoyancy compensation, and}$$
$$= 2.7 \text{ cm/s with buoyancy compensation}$$

Thus, the initial prototype design meets the minimum current requirement if buoyancy compensation is used.

A.3 DESIGN OF THE GUIDE CABLE BOTTOM WEIGHT

The guide cable will incline from the vertical because of its drag, and a weight is used at the bottom to reduce this inclination to an acceptable value. It can be easily shown from force balance consideration of the free body consisting of the cable, and the weight that the inclination at the top of the cable (where the inclination is maximum) is given by

$$\tan \phi_l = \frac{D_c + D_s + D_p + D_w}{W_c' + W_s' - L} \approx \frac{D_c}{W_c' + W_s'} \qquad (A.5)$$

where

ϕ_l = cable inclination at the top
D_c = drag of the cable
D_s = drag of the weight
D_p = drag of the payload housing
D_w = drag of the wing
W_c' = weight in water of the cable

W_s' = weight in water of the bottom weight
L = lift of the wing

The approximation on the right hand side is based on the assumption that the drag on the cable is the predominant drag. This assumption is justified below. The wing lift, L, is only transferred to the cable when the profiler is parked and is negligible in any case.

From force balance considerations on the weight the inclination at the bottom of the cable (where the inclination is minimum) is given by

$$\tan \phi_2 = \frac{D_s}{W_s'} \qquad (A.6)$$

where ϕ_2 is the cable inclination at the bottom.

The critical condition that determines the size of the bottom weight is the cable inclination at the top at the maximum operating current of 40 cm/s. This inclination should not exceed the pitch stop angle of 22 degrees, otherwise a positive angle of attack can not be attained by the wing. Fortunately, only a fraction of a degree angle of attack is needed to generate the required lift at these high currents. Also it is fortunate that cable angle at the bottom is not a design consideration at high current nor is cable angle at the top and bottom at minimum current operation a consideration. These angles are all small fractions of a degree.

A streamlined, 53 kg (in air) steel weight will limit the cable inclination to 20 degrees according to Equation (A.5). The details of the calculation are described below.

The following drag coefficients were used:

C_D = 1.8 for the cable
C_D = 0.06 for the weight
C_D = 0.04 for the profiler payload housing
C_D = 0.03 for the wing

These drag coefficients were estimated with appropriate consideration of Reynolds number. They are based on frontal reference areas except for the wing for which the planform area is used. Thus, for example, the drag of the cable is given by

$$D_c = C_{Dc} \tfrac{1}{2} \rho U^2 A_c$$

where

C_{Dc} = cable drag coefficient = 1.8
A_c = $L_c d_c$ = frontal area of the cable
L_c = length of the cable
d_c = diameter of the cable

We assumed a cable 300 m long and 0.5 cm in diameter, which gave a cable drag of 23 kg. A bottom weight frontal area of 70 cm^2 was assumed, which gave a drag of 3.6 gm. For the profiler housing shown in Figure A-3, with a frontal area of 1200 cm^2, the drag was calculated to be 41 gm. The wing shown in Figure A-3 with an area of 2900 cm^2 gave a drag of 72 gm. As stated earlier, the cable drag predominates, and the right hand side of Equation (A.5) was used. The cable assumed has a weight of 0.75 gm/m for a total weight of 23 kg. With a diameter of 0.5 cm, the weight in water is 16 kg. The steel bottom weight with a volume of 216 cm^2 weighs 53 kg, and its weight in water is 46 kg. The lift and weight in water of the profiler is only transmitted to the cable, when it is parked (held vertically at a stop). Of course, the weight in water of the profiler has been adjusted to a near zero value and thus does not appear in Equation (A.5). The lift of the profiler can also be neglected. The lift goes to zero at the critical cable tilt condition for which the angle of attack is zero. For tilt angles near this condition the angle of attack is small and produces insignificant lift compared to the cable weight in water. In fact the lift is insignificant for any angle of attack at the design maximum current speed.

Substituting the above values into Equation (A.5) gives a cable tilt angle of 20 degrees at the top. Substitution into Equation (A.6) gives a cable tilt angle of 0.004 degrees at the bottom of the cable.

If the above calculation is repeated for the minimum current case (U = 3 cm/s), the cable tilt at the top and the bottom is 0.3 and 0.0 degrees, respectively.

REFERENCE FOR APPENDIX

[A1] Lawford, J. A., and A. R. Beauchamp, "Low Speed Wind Tunnel Measurements on a Thin Sharp-Edged Delta Wing with 70 degree Leading-Edge Sweep, with Particular Reference to the Position of Leading Edge Vortex Breakdown," A.R.C.R.& M. No.3338, November 1961.